Journal of Inflammation Research

Dovepress
Taylor & Francis Group

Open Access Full Text Article

ORIGINAL RESEARCH

Effect of Sodium Butyrate and Sishen Pill Combination on Diarrhea with Kidney-Yang Deficiency Syndrome Was Associated with Intestinal Mucosal Microbiota and Immune Barrier

Jiaxin Di[1,2], Meifang Guo[1,2], Maijiao Peng[2,3], Leyao Fang[1,3], Junxi Shen[1,3], Nenqun Xiao[2,3], Zhoujin Tan[1,3]

[1]School of Traditional Chinese Medicine, Hunan University of Chinese Medicine, Changsha, People's Republic of China; [2]School of Pharmacy, Hunan University of Chinese Medicine, Changsha, People's Republic of China; [3]Hunan Key Laboratory of Traditional Chinese Medicine Prescription and Syndromes Translational Medicine, Changsha, People's Republic of China

Correspondence: Nenqun Xiao; Zhoujin Tan, Email xiaonenqun@sohu.com; tanzhjin@sohu.com

Purpose: To investigate the therapeutic mechanisms of sodium butyrate combined with SSP in treating diarrhea with kidney-yang deficiency syndrome, providing experimental evidence for the modern application of classical Chinese medicine formulas.

Methods: A mouse model of diarrhea with kidney-yang deficiency syndrome was established via adenine combined with *Folium sennae* gavage. After successful model establishment, the drug intervention groups were administered by gavage with 100% SSP decoction, 300 mg/mL sodium butyrate, and 100 mg/kg sodium butyrate + 50% SSP decoction, respectively. General physical conditions and organ indices were assessed. Serum tumor necrosis factor-α (TNF-α) and interleukin-6 (IL-6) levels, as well as colonic immunoglobulin A (sIgA) and mucin 2 (MUC2) levels, were determined via ELISA. Kidney and intestinal histology were evaluated via hematoxylin–eosin (HE) staining. The characteristics of the small intestinal mucosal microbiota under different interventions were analysed via 16S rRNA sequencing.

Results: Compared with natural recovery, the combination of 100 mg/kg sodium butyrate + 50% SSP significantly restored colonic sIgA levels ($p< 0.05$) and MUC2 levels, indicating an improvement in intestinal mucosal barrier function. Histological analysis revealed that the combination of 100 mg/kg sodium butyrate + 50% SSP improved renal inflammation and restored intestinal villus length and crypt depth. The combination therapy controlled the relative abundance of *Corynebacterium* while restoring *Dwaynesavagella* and *Megasphaera_A*. Correlation analysis indicated that *Mammaliicoccus* and *Corynebacterium* were significantly negatively correlated with sIgA and MUC2 levels and that their relative abundances were inhibited by the combination therapy.

Conclusion: Sodium butyrate enhanced the therapeutic efficacy of SSP. The combination therapy effectively repaired damaged kidneys and intestines and alleviated diarrhea with kidney-Yang deficiency syndrome by modulating the relative abundance of intestinal microbiota and enhancing intestinal immunity as well as mucosal barrier function. The interaction between the intestinal microbiota and intestinal mucosal protective factors may be a key mechanism in the combined treatment of diarrhea with kidney-yang deficiency syndrome.

Keywords: diarrhea with kidney-yang deficiency syndrome, mucosal barrier, intestinal microbiota, Sishen pill, sodium butyrate, short-chain fatty acids

Introduction

Diarrhea is a globally prevalent condition that encompasses a variety of diseases. Traditional Chinese Medicine (TCM) categorizes diarrhea into distinct syndromic types on the basis of its etiology, pathogenesis, and clinical manifestations.[1] Among these, diarrhea with kidney-yang deficiency syndrome is one of the more common syndromes. According to TCM theory, the kidneys are the root of Yang energy, which supports the spleen's transformation and transportation

Received: 19 January 2025
Accepted: 16 July 2025
Published: 4 August 2025

functions—critical for water metabolism and digestive health. Diarrhea with kidney-yang deficiency syndrome is primarily caused by insufficient kidney-yang and the gradual decline of spleen and stomach function, resulting in impaired digestive activity. Spleen-Yang is dependent on kidney-yang as its congenital foundation; only when kidney-yang is abundant can the spleen be adequately warmed. At the same time, kidney-yang relies on the Qi and blood generated by the spleen and stomach for nourishment. When kidney-yang is deficient, this leads to insufficient warmth and dysfunction in the spleen and intestines, resulting in poor absorption, increased fluid retention, and ultimately diarrhea. Prolonged diarrhea further impairs spleen-yang, hindering the replenishment of kidney-yang, which in turn leads to dysfunction of both organs and persistent diarrhea. The complexity and diversity of pathogenic factors present significant challenges in understanding their underlying mechanisms, thereby hindering progress in the development of effective therapeutic strategies. Consequently, elucidating the pathogenesis of diarrhea in patients with kidney-yang deficiency syndrome and identifying efficacious treatments are critically important for maintaining human health.

With the advancement of high-throughput sequencing technologies for the intestinal microbiota, researchers have increasingly recognized the close relationship between alterations in the structure and function of the intestinal microbiota and the onset and recovery of systemic diseases, including those affecting the nervous, endocrine, immune, and digestive systems. The intestinal microbiota plays a pivotal role in maintaining human health.[2–5] Studies have shown significant differences in the intestinal microbiota composition between diarrheal mice with kidney-yang deficiency syndrome and normal mice. The former exhibits elevated concentrations of the harmful microbial metabolite Trimethylamine-N-oxide (TMAO), which disrupts intestinal barrier function and contributes to intestinal inflammation.[6] Traditional Chinese medicines (TCMs), which are predominantly administered orally, directly interact with the gastrointestinal tract, modulating the composition and metabolism of the intestinal microbiota, protecting the intestinal mucosa, and thereby intervening in the pathogenesis and progression of diarrhoeal diseases.[7] Sishen Pill (SSP), a classic prescription for treating diarrhea in patients with kidney-yang deficiency syndrome, warm the kidney, strengthen the spleen, consolidate the intestines, and alleviate diarrhea.[8] SSP has been shown to restore the intestinal microbiota balance and maintain intestinal barrier integrity, thereby addressing intestinal disorders. Active metabolites in SSP, such as psoralen, evodiamine, and schisandrin, effectively control intestinal inflammation and demonstrate therapeutic potential in conditions such as irritable bowel syndrome and ulcerative colitis.[9–11] In our previous research, we found that SSP restored the taxonomic composition and microbial communities of the intestinal mucosa in diarrheal mice with kidney-yang deficiency syndrome. By reducing the relative abundance of bacteria such as *Firmicutes* and *Succinatimonas hippei*, SSP lowered intestinal TMAO levels, thereby alleviating diarrhea symptoms. Moreover, it improved renal fibrosis in these mice, contributing to their recovery.[12] Additionally, SSP enhances intestinal barrier function through mechanisms such as promoting the secretion of intestinal secretory immunoglobulin A (sIgA) or modulating the expression of colonic mucin 2 (MUC2), further mitigating diarrhea.[13,14]

Short-chain fatty acids (SCFAs) are also involved in the development of diarrhea in patients with kidney-yang deficiency syndrome. Studies have demonstrated that SSP restores the levels of propionate, butyrate, and isobutyrate and isovalerate in the intestinal contents of diarrheal mice with kidney-yang deficiency syndrome while reducing the levels of acetate and valerate.[15] Among SCFAs, butyrate is particularly important because of its ability to regulate the intestinal microbiota balance, inhibit the growth of harmful bacteria, control intestinal inflammation, and enhance intestinal mucosal immune function.[16] Research has shown a positive correlation between butyrate levels and IgA concentrations, suggesting that butyrate strengthens mucosal immunity and prevents bacterial translocation under inflammatory conditions.[17] Furthermore, butyrate improves the intestinal microbiota composition, increases the villus length, and reduces the crypt depth.[18] The appropriate dosage of sodium butyrate is also critical. Studies indicate that sodium butyrate is most effective at concentrations between 100 mg/kg and 400 mg/kg, alleviating neutrophil infiltration and mitigating colon shortening in mice with DSS-induced colitis. However, dosages exceeding 500 mg/kg can exacerbate colonic injury in mice.[19]

With increasing research on TCM and intestinal microecology, an increasing number of studies have shown that the combination of TCM and microbiota-based therapies can enhance therapeutic efficacy. For instance, 25% ultra-micro Qiweibaizhusan + 25% yeast had the best compatibility, achieving the same efficacy as the full dose of traditional decoctions while reducing the use of medicinal materials.[20] Building on prior models established by our research group, this study

investigated the combined therapeutic effects of sodium butyrate and SSP. Focusing on the intestinal microbiota, this study examined changes in TNF-α, IL-6, sIgA, and MUC2 levels in mice, alongside histological observations of renal and intestinal tissues. This approach aims to evaluate the efficacy of the combined treatment for diarrhea with kidney-yang deficiency syndrome. This study aimed to elucidate the mechanisms underlying the therapeutic effects of sodium butyrate and SSP, particularly their roles in intestinal mucosal barrier function and microbial composition. These findings are expected to provide novel insights into the use of SSP for treating diarrhea in patients with kidney-yang deficiency syndrome.

Materials and Methods

Materials

Experimental Animals and Housing Conditions

Fifty male KM mice (SPF grade), weighing 18–22 g, were purchased from Hunan Silaike Jingda Laboratory Animal Co., Ltd. (Licence No. SCXK (Xiang) 2019–0004). The mice were housed at the Animal Experiment Center of Hunan University of Chinese Medicine (Laboratory Licence No. SYXK (Xiang) 2019–0009). The experiment was approved by the Animal Ethics and Welfare Committee of Hunan University of Chinese Medicine (Approval No. HNUCM21-2403-43), and all programs and operations of the experiment were conducted in strict compliance with the National Laboratory Animal Welfare Standards: Laboratory Animal—Guideline for Ethical Review of Animal Welfare (GB/T 35892–2018). The breeding feed used for the mice in this study was provided by the Experimental Animal Center of Hunan University of Chinese Medicine and manufactured by Beijing Huafukang Bioscience Co., Ltd. The main components of the feed included crude protein (≥20%), crude fat (≥4%), crude fibre (≤5%), crude ash (≤8%), moisture (≤10%), lysine (≥1.3%), calcium (0.6–1.8%), phosphorus (0.6–1.2%), and salt (0.3–0.8%), ensuring cleanliness and contamination-free conditions. The feed licence number is Jing Feed Certificate: (2019) 06076.

Experimental Drugs and Preparation

Adenine (Biofroxx, Germany, Batch No. EZ7890C450) was used to prepare a 5 mg/mL suspension in sterile water. The suspension was freshly prepared daily, protected from light, and stored appropriately.

Folium sennae (Bozhou Huqiao Pharmaceutical Co., Ltd., Batch No. 2111090022) was processed into a decoction by soaking the leaves and heating them in a water bath. The mixture was filtered and concentrated to yield a decoction containing 1 g/mL raw herbs and stored in a refrigerator at 4 °C.

Sishen Pill is composed of *Psoralea corylifolia* L (Hunan Junhao Traditional Chinese Medicine Decoction Pieces Science and Trade Co., Ltd., NO.23100112), *Myristica fragrans* Houtt (Hunan Hengyue Traditional Chinese Medicine Decoction Pieces Co., Ltd., NO. 23083107), *Euodia rutaecarpa (Juss.)* Benth (Hunan Rongkang Traditional Chinese Medicine Decoction Pieces Co., Ltd., 230801), *Schisandra chinensis (Turcz.)* Baill (Haozhou Yonggang Decoction Pieces Factory Co., Ltd., A231031), *Ziziphus jujuba* Mill (Hunan Xinshen Zhilin Traditional Chinese Medicine Decoction Pieces Co., Ltd., 2310001), *Zingiber officinale* Roscoe, a total of 39 g, at a ratio of 4:2:1:2:2:2:2. The drug was weighed according to the formula ratio, soaked in 300 mL of water for 30 min, boiled and then turned to a simmer for 30min, and filtered the drug solution with gauze. The remaining residue was decocted with 200 mL of water according to the same procedure, filtered, mixed twice, and concentrated into a decoction of Sishen Pill containing 0.29 g/mL crude drug,[15] which was stored at 4 °C for later use. SSP and sodium butyrate (Shanghai Aladdin Biochemical Technology Co., Ltd., NO. I2313563) were combined in proportion.

Kits

All the ELISA kits used were purchased from Jiangsu Jingmei Biotechnology Co., Ltd.: Tumor Necrosis Factor-α (TNF-α) ELISA Kit (Cat. No. JM-02415M2). Interleukin-6 (IL-6) ELISA Kit (Cat. No. JM-02446M2). Mucin 2 (MUC2) ELISA Kit (Cat. No. JM-1138M2). Secretory Immunoglobulin A (sIgA) ELISA Kit (Cat. No. JM-02713M2).

Methods

Model Establishment

After 4 days of adaptive feeding, 50 Kunming mice were randomly divided into a normal group (CC, n = 10) and a model group (n = 40) via a random number table A diarrhea with kidney-yang deficiency syndrome model was induced in the model group via the combination of adenine and a decoction of *Folium sennae*.[21] The modelling process lasted for 14 days. The model group received adenine suspension (50 mg/(kg·d), 0.4 mL/each, once/d) via gavage for 14 consecutive days. Beginning on day 8, *Folium sennae* decoction (10 g/(kg·d), 0.4 mL/mouse, once daily) was administered for 7 consecutive days. During the same period, the normal group was gavaged with an equal volume of sterile water at the same frequency.

Grouping and Administration Methods

After successful model establishment, the model factors were discontinued, and the model group was subdivided into four groups for treatment: the natural recovery group (NR), 100% SSP group (SSP), sodium butyrate combined with SSP group (CR), and sodium butyrate group (CB). Research has indicated that the combination of 100 mg/kg sodium butyrate and 50% SSP has significant efficacy against diarrhea in patients with kidney-yang deficiency syndrome; therefore, this combination was selected for intervention. The SSP group received SSP decoction (5 g/(kg·d), 0.35 mL/mouse, twice daily) via gavage for 7 consecutive days. The other treatment groups received the corresponding drug solutions in equal volumes and at the same frequency. The normal group and natural recovery group were gavaged with an equal volume of sterile water at the same frequency. The SSP gavage dosage was determined on the basis of previous studies conducted by the research team.[21]

Model Evaluation Criteria

Evaluation criteria for the model were established on the basis of the clinical manifestations of diarrhea with kidney-yang deficiency syndrome. These criteria included measuring rectal temperature and body weight and observing behavioral changes to assess symptoms such as cold extremities, reduced body temperature, weight loss, and lethargy. The fecal water content was determined to evaluate the severity of diarrhea.[21]

Measurement of Rectal Temperature, Body Weight, and Fecal Water Content

The rectal temperature and body weight of the mice were measured on days 1, 7, 14, 17, and 21 of the experiment. Fresh fecal samples were collected on days 1, 14, and 21. The wet weight of the feces was recorded, and the samples were dried at 110 °C to a constant weight, after which their dry weight was measured (fecal water content was analyzed as a descriptive symptom marker, not for statistical comparison). The fecal water content (%) was calculated via the following formula:

Fecal moisture content (%)= (wet weight–dry weight) (g)/wet weight (g) ×100%

Measurement of Organ Index

The intact spleen, thymus, and liver were collected, and excess adipose tissue was removed. The organs were blotted dry with filter paper to remove surface blood before weighing. The organ index (%) was calculated via the following formula:

$$\text{Organ index (\%)} = \text{Organ mass (g)}/\text{Body mass (g)} \times 100\%$$

Measurement of TNF-α, IL-6, MUC2, and sIgA

Enzyme-linked immunosorbent assay (ELISA) was used to measure the levels of TNF-α and IL-6 in the serum samples and the levels of MUC2 and sIgA in the colon samples.

Blood samples from the mice in each group were collected into 1.5 mL EP tubes, left to stand at room temperature, and then centrifuged at 3000 rpm for 10 minutes. The supernatant was collected and used for TNF-α and IL-6 detection according to the ELISA kit instructions.

Colon tissue samples from each group of mice were collected into 1.5 mL EP tubes, homogenized with 3 grinding beads and a specific ratio of physiological saline, and then centrifuged at 3000 rpm for 10 minutes. The supernatant was collected and used for MUC2 and sIgA detection according to the ELISA kit instructions.

Histopathological Observation of Kidney and Small Intestine Tissue

Kidney and small intestine tissues from the mice were fixed in paraformaldehyde, dehydrated via a gradient series of alcohols and cleared in xylene. After being embedded in paraffin, tissue sections were prepared and stained with hematoxylin and eosin (HE). The pathological changes in the intestine and kidney tissues were observed under a light microscope, and images were captured. Using ImageJ software, the height of the intestinal villi and the depth of the crypts were measured for each group of mice to assess the activity and function of intestinal stem cells.

DNA Extraction and 16S rRNA High-Throughput Sequencing

① Sample collection: In a sterile environment, the small intestine tissue of each mouse was collected, the intestinal wall was washed with normal saline, and the small intestinal mucosa was scraped with a coverslip, placed in a 1.5 mL EP tube, placed in liquid nitrogen for quick freezing, and then stored in groups at −80 °C.

② Extraction and detection of total microbial DNA: After pretreatment of the samples, nucleic acids were extracted via an OMEGA Soil DNA Kit (D5635-02) (Omega Bio-Tek, Norcross, GA, USA). The extracted DNA was judged by molecular size via 0.8% agarose gel electrophoresis, and the DNA was quantified via a Nanodrop (Thermo Scientific, NC2000).

③ PCR amplification and recovery and purification of its products: PCR amplification was performed via specific primers in the V3–V4 region of bacterial 16S rRNA, with the forward primer sequence 338 F (5′-ACTCCTACGGGAGGCAGCA-3′) and the reverse primer sequence 806 R (5′-GGACTACHVGGGTWTCTAAT-3′). The PCR products were detected via 2% agarose gel electrophoresis and purified via the Axygen Gel Recovery Kit.

④ PCR product quantification: The Quant-it PicoGreen dsDNA Assay Kit is used to quantify the recovered PCR amplification products. The samples were mixed proportionally according to the amount of data required for sequencing each sample.

⑤ Library construction and sequencing: An Illumina TruSeq Nano DNA LT Library Prep Kit was used for library construction, and after quality inspection and quantification of the library, the qualified libraries were sequenced on Illumina NovaSeq (PE250 double-ended sequencing) or Illumina MiSeq (PE300 double-ended sequencing) instruments. The sequencing work was carried out at Shanghai Personal Biotechnology Co., Ltd., and the sequencing data of the intestinal mucosal microbiota were uploaded to the NCBI database under the number PRJNA1121031.

Bioinformatics Analysis

① Species annotation: Paired-end sequencing of community DNA fragments was performed via the Illumina platform to obtain raw data. The primer fragments of the cut-out sequence were called to be called to trim-paired, and the sequences of unmatched primers were discarded. DADA2 is then called through qiime dada2 denoise-paired for data processing, such as quality control, denoising, splicing, and chimera de-chimeraization. The obtained ASV (Amplicon Sequence Variant) feature sequences were compared with the database reference sequences to obtain the taxonomic information corresponding to each ASV. QIIME 2 software was used to randomly extract the serial numbers of each sample in the ASV abundance matrix at different depths, and species annotation was performed via the naive Bayes classifier. The sparse curves were plotted with the extracted serial numbers and the corresponding ASV numbers at each depth, and the quality of the sequencing data was evaluated by the sparse curves and abundance grade curves.

② Alpha diversity analysis: Alpha diversity refers to the indicators of the richness and diversity of species in locally homogeneous habitats. The Chao1 index, observed species index, Shannon index and Simpson index of each sample were calculated via QIIME 2 software, and the abundance and uniformity of ASVs among different samples were compared.

③ Beta diversity index analysis: The beta diversity index reflects the differences in microbial communities among samples. Principal coordinate analysis (PCoA) was used to reduce the dimensionality of the data, and the main trends of the data changes are displayed.

④ Species difference and Feature Microbiota Analysis: The VennDiagram package and R script were used to generate petal maps or Venn diagrams to visualize the common species and unique species between samples. The composition and abundance tables of each sample at different taxonomic levels were obtained via QIIME2 software and are presented in the form of bar graphs. Linear discriminant analysis and linear discriminant analysis effect size (LEfSe)

analysis were used to detect the differential abundance among different taxa. Random forest analysis was performed on samples from different groups via the default settings of QIIME2.

⑤ Correlation analysis: Spearman correlation coefficients between characteristic bacteria and IL-6, TNF-α, MUC2 and sIgA were calculated. Cytoscape 3.7.2 software was used to construct related networks, and the synergistic/competitive relationship between the two networks was determined. Redundancy analysis (RDA) was used to study the effects of the interaction between sodium butyrate and Sishen pill on the characteristic microflora of the intestinal mucosa and environmental factors in mice with kidney yang deficiency syndrome.

⑥ Functional prediction analysis: PICRUSt2 was used to predict the functional abundance of samples in the KEGG database, and LEfSe analysis was performed to obtain metabolic pathways with different abundances between groups.

Statistical Analysis

SPSS 25 was used for statistical analysis, and the data of each group are expressed as the mean ± standard deviation. If the data between multiple groups were in accordance with the normal distribution and homogeneity of variance, one-way ANOVA was used, otherwise the Kruskal–Wallis *H*-test was used. $p< 0.05$ indicated significant differences, and $p< 0.01$ indicated significant differences.

Results

Effects of SSP Combined with Sodium Butyrate on General Behavior, Body Weight, and Anal Temperature in Mice

As shown in Figure 1A, mice in the normal group are active and responsive, and the bedding in the cage is relatively dry. In contrast, mice in the natural recovery group showed obvious huddling behavior in the corners of the cage due to cold intolerance. These mice appeared lethargic, had delayed responses, reduced activity, and lost curiosity about their

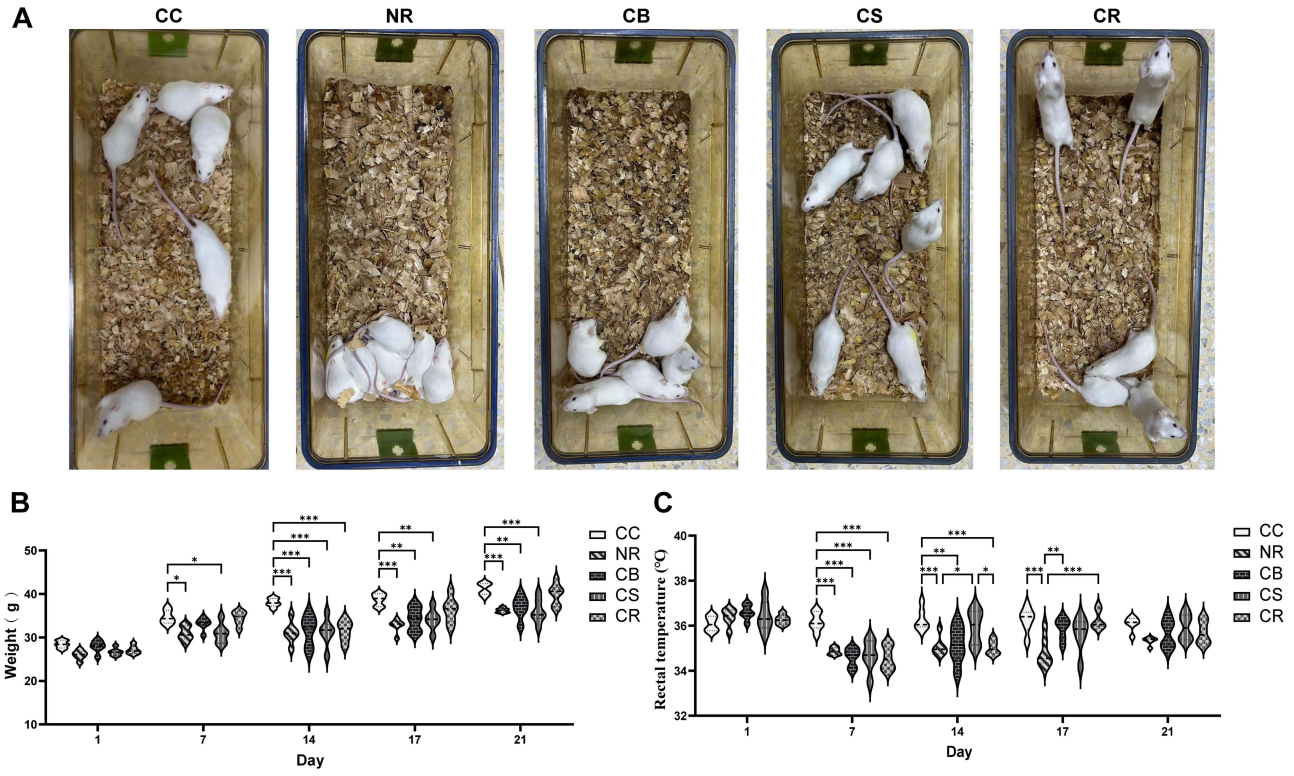

Figure 1 Effects of SSP combined with sodium butyrate on the general behavior, body weight, and rectal temperature of mice.
Notes: (**A**) General behavior; (**B**) Body weight; (**C**) Rectal temperature. *p<0.05; **p<0.01; ***p<0.001. CC: Normal group; NR: Natural recovery group; CB: Sodium Butyrate group; CS: SSP group; CR: 100 mg/kg sodium butyrate + 50% SSP group.

surroundings. Additionally, their bedding was noticeably wet and darkened as a result of persistent diarrhea. In comparison, mice in the drug-treated groups showed improvements in both activity levels and reduced huddling behavior.

As shown in Figure 1B, on the final day of modelling, the body weight of each model group was significantly lower than that of the normal group ($p<0.001$). After treatment, the body weight in the group treated with 100 mg/kg sodium butyrate + 50% SSP recovered to a level that was not significantly different from that of the normal group ($p>0.05$), whereas a significant difference ($p<0.01$) remained between the other treatment groups and the normal group. Figure 1C shows that the model altered the rectal temperature of the mice. On the 7th day of the experiment, the rectal temperature of all the model groups was significantly lower than that of the normal group ($p<0.001$), and these differences persisted until the end of the modelling period. After the initiation of treatment, the rectal temperature of the diarrheal mice with kidney-yang deficiency syndrome in each treatment group began to recover. On the 3rd day of treatment, the natural recovery group still showed a highly significant difference compared with the normal group ($p<0.001$). However, the rectal temperatures of the mice in the sodium butyrate group and the 100 mg/kg sodium butyrate + 50% SSP group were significantly higher than those in the natural recovery group ($p<0.01$, $p<0.001$). On the final day of treatment, although the rectal temperature in the natural recovery group remained low, no significant differences were observed among the groups ($p>0.05$). Although the rectal temperatures in all the groups recovered after the cessation of modelling, the recovery was faster and more pronounced in the treatment groups. In particular, the rectal temperature in the 100 mg/kg sodium butyrate + 50% SSP group was highly significantly different from that in the natural recovery group as early as the 3rd day of treatment ($p<0.001$). These findings suggest that the SSP group, sodium butyrate group, and their combination all have certain efficacy in improving the symptoms of diarrhea with kidney-yang deficiency syndrome in mice, with the combined use of sodium butyrate and SSP potentially achieving superior therapeutic effects.

Effects of SSP Combined with Sodium Butyrate on Mouse Feces

On the 3rd day after gavage with *Folium sennae* decoction, the mice began to exhibit symptoms of loose stools and diarrhea: feces became lighter in color, easily deformed when picked up with tweezers, and left noticeable water stains when pressed onto filter paper. The perianal areas of the mice appeared moist with fecal adhesion, and the bedding turned dark with a strong odor. The fecal water content in the model groups increased sharply, whereas it remained stable in the normal group. After the cessation of modelling and the initiation of treatment, the fecal water content decreased to varying degrees. The reduction was more pronounced in the SSP group and the 100 mg/kg sodium butyrate + 50% SSP group, with the fecal water content of the combined treatment group closely approaching that of the normal group. In contrast, the natural recovery group presented a slower reduction in the fecal water content, which remained higher than that of the other groups. Post-treatment, the mice had clean perianal areas, the fecal color returned to normal, and the water on the filter paper had disappeared. However, some of the mice in the natural recovery group still had softer feces and moist perianal areas (Figure 2A and B).

Effects of SSP Combined with Sodium Butyrate on the Organ Index in Mice

As a preliminary indicator of immune function, the organ index can reflect changes in the immune capacity of the body to a certain extent.[22] As shown in Figure 3A and B, compared with those in the normal group, the thymus and spleen indices in the natural recovery group were significantly elevated ($p<0.05$), whereas those in the other treatment groups recovered to levels that were not significantly different from those in the normal group ($p>0.05$). The liver index in the natural recovery group, sodium butyrate group, and SSP group were significantly lower than those of the normal group ($p<0.001$, $p<0.01$, $p<0.001$). After treatment with 100 mg/kg sodium butyrate + 50% SSP, the liver index recovered and was not significantly different from that of the normal group ($p>0.05$).

Effects of SSP Combined with Sodium Butyrate on Serum TNF-α and IL-6 Levels and Colonic sIgA and MUC2 Levels

As shown in Figure 4A and B, the serum levels of TNF-α and IL-6 were measured. Compared with those in the normal group, the TNF-α levels in the natural recovery group were significantly lower ($p<0.01$), while the TNF-α levels increased

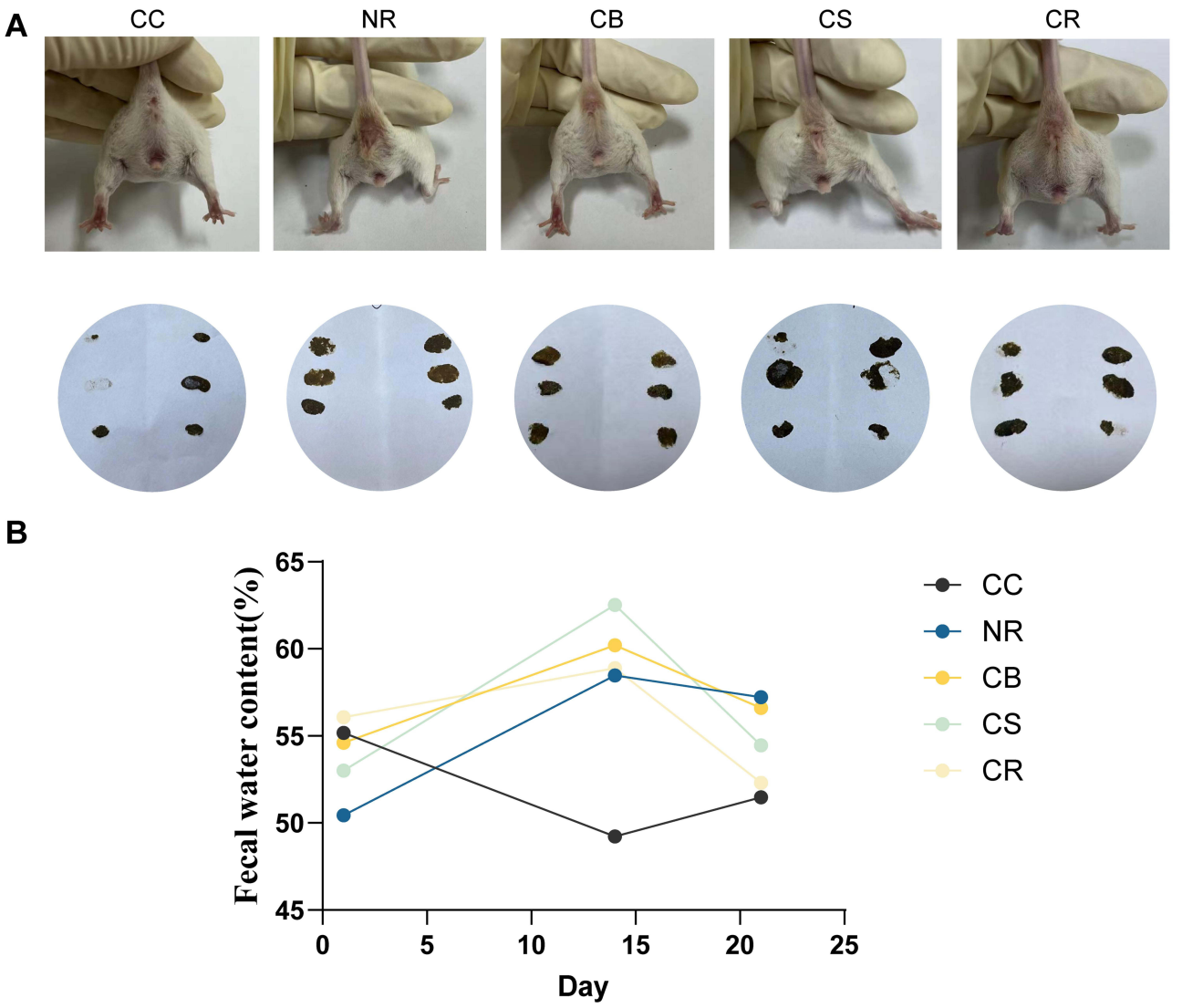

Figure 2 Effects of SSP combined with sodium butyrate on the diarrhea status of mice.
Notes: (**A**) Perianal cleanliness and fecal characteristics in each group; (**B**) Fecal water content (Data represent single measurements per time point for symptom trend evaluation.). CC: Normal group; NR: Natural recovery group; CB: Sodium Butyrate group; CS: SSP group; CR: 100 mg/kg sodium butyrate + 50% SSP group.

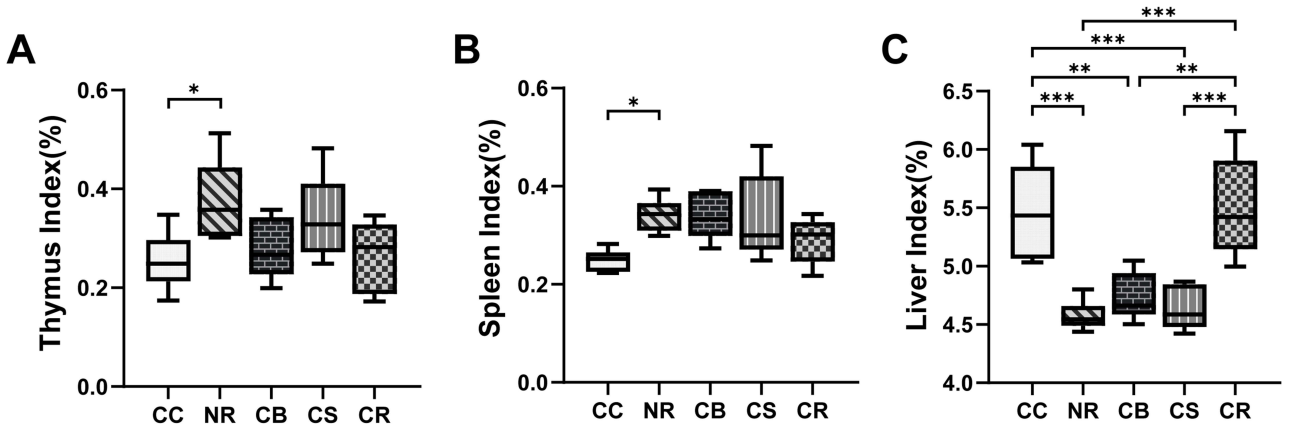

Figure 3 Effects of SSP combined with sodium butyrate on the organ index in mice.
Notes: (**A**) Thymus index; (**B**) Spleen index; (**C**) Liver index. *p<0.05; **p<0.01; ***p<0.001. CC: Normal group; NR: Natural recovery group; CB: Sodium Butyrate group; CS: SSP group; CR: 100 mg/kg sodium butyrate + 50% SSP group.

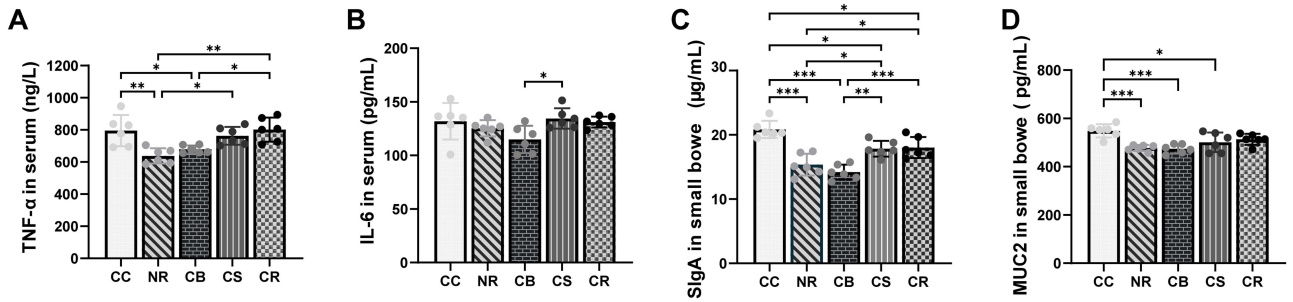

Figure 4 Effects of SSP and sodium butyrate combination therapy on serum TNF-α and IL-6 levels and colonic sIgA and MUC2 levels in mice.
Notes: (**A**) TNF-α levels; (**B**) IL-6 levels; (**C**) sIgA levels; (**D**) MUC2 levels. **p*<0.05; ***p*<0.01; ****p*<0.001. CC: Normal group; NR: Natural recovery group; CB: Sodium Butyrate group; CS: SSP group; CR: 100 mg/kg sodium butyrate + 50% SSP group.

sequentially in the sodium butyrate group, SSP group, and 100 mg/kg sodium butyrate + 50% SSP group. There were no significant differences in the IL-6 levels between the other groups and the natural recovery group ($p>0.05$).

As shown in Figure 4C and D, the levels of sIgA and MUC2 in the colonic tissue were assessed. Compared with those in the normal group, the sIgA and MUC2 levels in the natural recovery group were significantly lower ($p<0.001$). After treatment, the sIgA levels in the SSP group and the 100 mg/kg sodium butyrate + 50% SSP group increased significantly, with notable differences compared with those in the natural recovery group ($p<0.05$). Additionally, the MUC2 levels in the colonic tissue of the 100 mg/kg sodium butyrate + 50% SSP group recovered to levels not significantly different from those in the normal group ($p>0.05$). These findings suggest that among the three treatment groups, the 100 mg/kg sodium butyrate + 50% SSP group may provide stronger repair and protective effects on the intestinal mucosa of diarrheal mice with kidney-yang deficiency syndrome.

Effects of SSP and Sodium Butyrate Combination Therapy on the Small Intestine and Kidney of Mice

Figure 5A and B illustrate the structural changes in the small intestines of the mice across the experimental groups. In the normal group, the intestinal villi and lamina propria were intact. In the natural recovery group, the lamina propria thinned, and the intestinal villi atrophied, with the villus length (422.014 ± 76.095 μm) significantly shorter than that in the normal group (485.296 ± 45.499 μm). The villus length in the SSP group and the 100 mg/kg sodium butyrate + 50% SSP group recovered. Crypt depth reflects the cell maturation rate and nutrient absorption capacity. Crypts in the natural recovery group exhibited loss and elongation, with a significantly greater crypt depth than those in the normal group did ($p< 0.001$). The crypt depth in the other treatment groups recovered to levels that were not significantly different from those in the normal group ($p > 0.05$). Compared with the natural recovery group, the sodium butyrate group and the 100 mg/kg sodium butyrate + 50% SSP group presented significantly reduced crypt depth ($p< 0.001$).

Figure 5C shows the histopathological results of the kidneys from each group of mice. In the normal group, the renal tubules had even lumens, with no glassy degeneration in the tubular walls and no inflammatory cell infiltration in the renal interstitium. In the natural recovery group, localized renal tissue was disorganized, with significantly dilated renal tubules, chronic inflammatory cell infiltration, and partial adhesion of glomerular capsules, along with narrowed capillary lumens and glomerular capsule lumens. In the treatment groups, the sizes of the glomeruli and renal tubules generally recovered. However, in the SSP group, the glomerular capsule lumen remained narrowed, and both the SSP and sodium butyrate groups still exhibited chronic inflammatory cell infiltration. In contrast, the 100 mg/kg sodium butyrate + 50% SSP group showed good recovery, with a notable improvement in inflammatory cell infiltration.

https://doi.org/10.2147/JIR.S518370

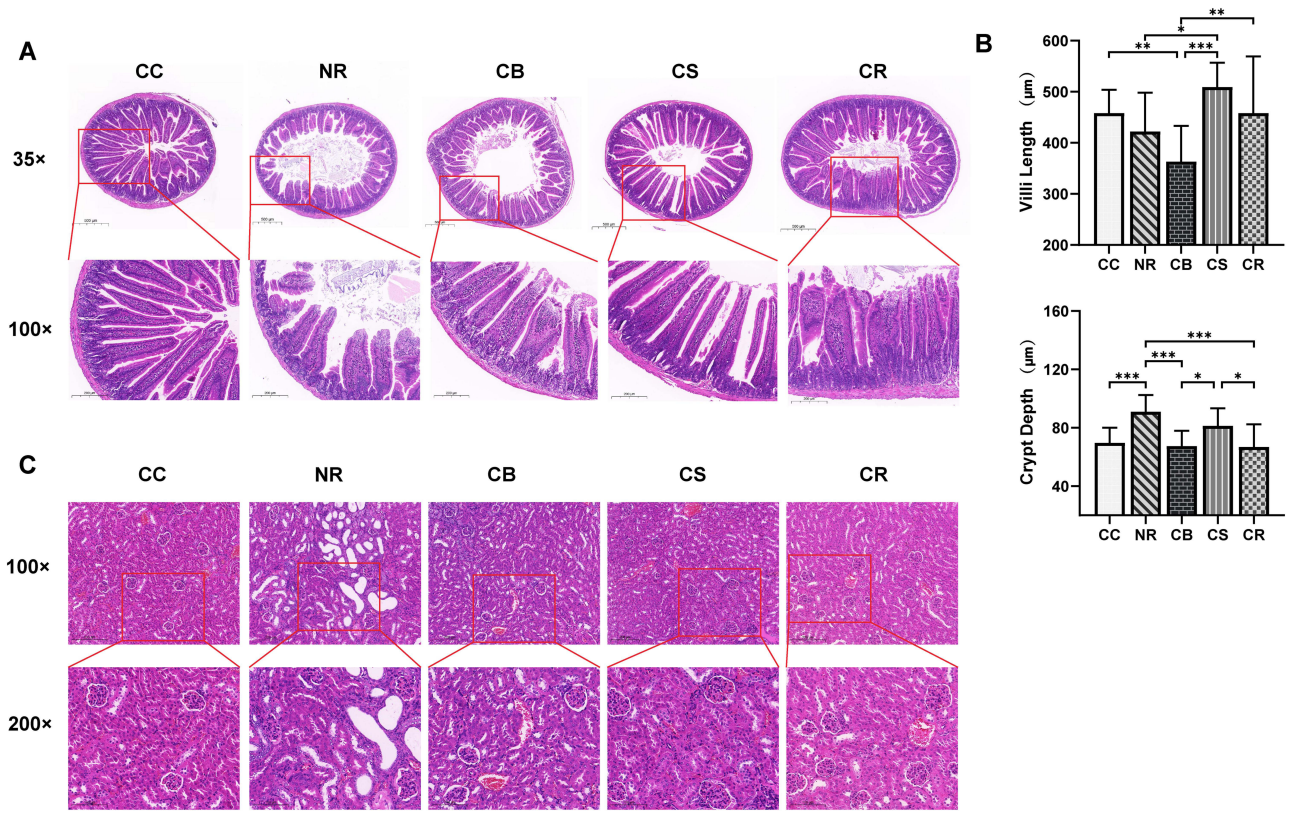

Figure 5 Effects of Sishen Pill combined with sodium butyrate on the structure of the kidney and Small Intestine in Mice with kidney-yang Deficiency Syndrome.
Notes: (**A**) HE section of small intestine; (**B**) Changes in small intestinal villus length and crypt depth in each group; (**C**) Renal HE-stained sections. *p<0.05; **p<0.01; ***p<0.001. CC: Normal group; NR: Natural recovery group; CB: Sodium Butyrate group; CS: SSP group; CR: 100 mg/kg sodium butyrate + 50% SSP group.

Effects of the SSP and Sodium Butyrate Combinations on the Intestinal Microbiota of Mice

Effects on the Diversity of the Intestinal Mucosal Microbiota in Mice

Alpha diversity reflects the richness and diversity of microbial communities within a sample. The Chao1 index and Observed_species index were used to evaluate species richness, whereas the Shannon and Simpson indices were used to assess species diversity. As shown in Figure 6A, compared with those in the normal group, the Chao1 and Observed_species indices in the natural recovery group increased slightly. In contrast, these indices decreased in the sodium butyrate group, SSP group, and 100 mg/kg sodium butyrate + 50% SSP groups. Compared with those of the normal group, the Shannon and Simpson indices of all the groups also tended to decrease. However, no significant differences were observed among the groups (p > 0.05). These findings suggest that, in diarrhea with kidney-yang deficiency syndrome mice, treatment with sodium butyrate, SSP, or their combination modestly altered the internal microbial alpha diversity, which was primarily reflected in the reduction in intestinal microbial richness and diversity.

Beta diversity highlights differences in microbial community composition between samples. In the PCoA analysis, the closer two points are on the coordinate axes, the more similar the community composition is between the corresponding samples. As shown in Figure 6B, there was a certain degree of difference in the community composition of the samples in each group. After treatment, sample clustering was observed, with the sodium butyrate group and the 100 mg/kg sodium butyrate + 50% SSP group showing projection regions that did not overlap with those of the natural recovery group. The samples from the 100 mg/kg sodium butyrate + 50% SSP group were tightly clustered within the projection area of the normal group and were farther from the natural recovery group. As shown in Figure 6C, PERMANOVA analysis revealed significant differences between the normal and SSP groups (p=0.019) and between

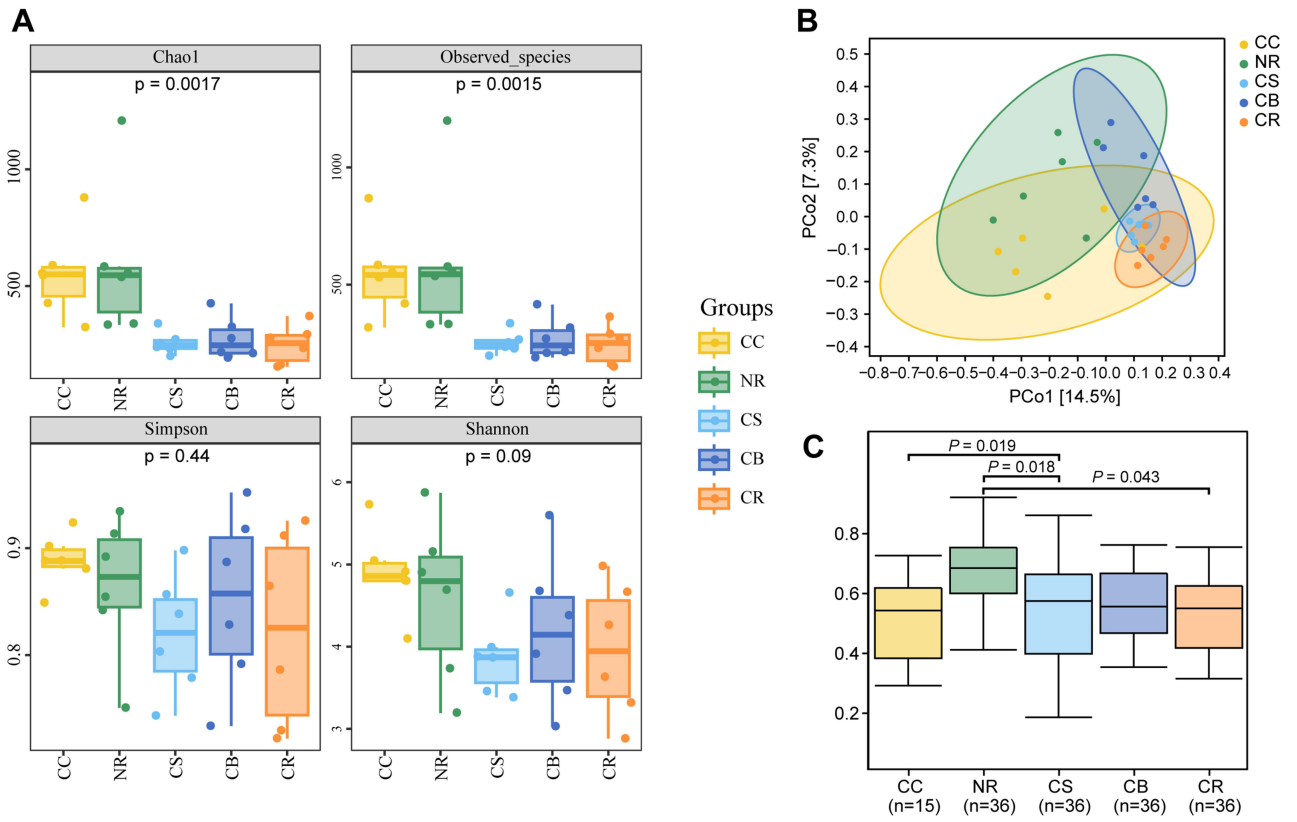

Figure 6 Effects of the Sishen pill combined with sodium butyrate on the diversity of the intestinal mucosal microbiota in diarrheal mice with kidney-yang deficiency syndrome.
Notes: (**A**) Alpha diversity indices; (**B**) Principal Coordinates Analysis; (**C**) PERMANOVA analysis. *p<0.05; **p<0.01; ***p<0.001. CC: Normal group; NR: Natural recovery group; CB: Sodium Butyrate group; CS: SSP group; CR: 100 mg/kg sodium butyrate + 50% SSP group.

the natural recovery group and both the SSP group (p=0.018) and the 100 mg/kg sodium butyrate + 50% Sishen Pill group (p=0.043). These results indicate that the 100 mg/kg sodium butyrate + 50% SSP group and the SSP group had significant effects on altering the intestinal mucosal microbiota in diarrheal mice with kidney-yang deficiency syndrome. This alteration may play a positive role in restoring intestinal homeostasis.

Effects of SSP Combined with Sodium Butyrate on Dominant Bacterial Populations in the Intestinal Mucosa of Mice

Different treatment regimens can alter the composition of the intestinal mucosal microbiota in mice. We selected the top 10 taxa in terms of abundance at the phylum and genus levels for statistical analysis, and the results are presented as bar charts. As shown in Figure 7A, at the phylum level, Firmicutes was the predominant phylum across all groups. The Actinobacteria was the second most abundant phylum, followed by Bacteroidota, which ranked third. These three phyla constituted a significant proportion of the microbiota in all five experimental groups. Figure 7B illustrates the changes in dominant genera across groups. The relative abundance of *Ligilactobacillus* decreased in the natural recovery group but increased in the sodium butyrate group and the 100 mg/kg sodium butyrate + 50% SSP combination group. *Dwaynesavagella* was the dominant genus across all the groups. Compared with that in the natural recovery group, the relative abundance of *Dwaynesavagella* increased by 18.96%, 11.34%, and 13.56% in the SSP group, sodium butyrate group, and 100 mg/kg sodium butyrate + 50% SSP combination group, respectively (Figure 7C). *Megasphaera_A* was the second most abundant genus, with relative abundances increasing by 9.86%, 2.49%, and 9% in the SSP group, sodium butyrate group, and 100 mg/kg sodium butyrate + 50% SSP combination group, respectively, compared with those in the natural recovery group. However, the differences in these two genera among the groups were

https://doi.org/10.2147/JIR.S518370

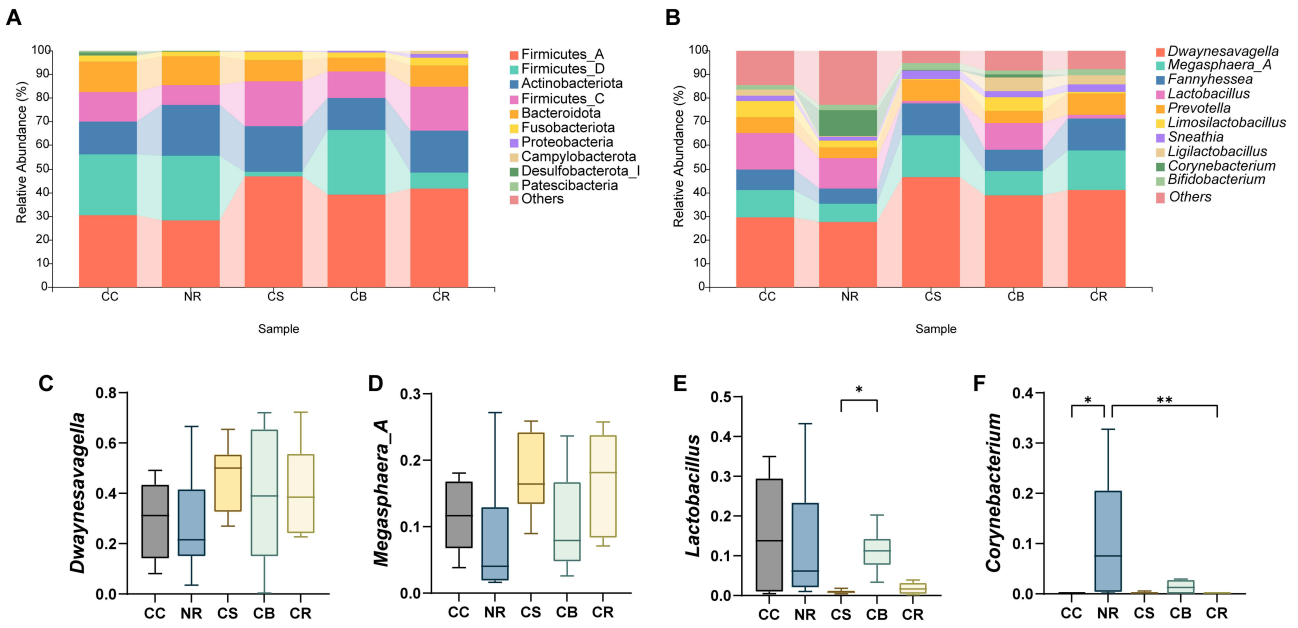

Figure 7 Effects of SSP combined with sodium butyrate on the dominant genera of the small intestinal mucosal microbiota in diarrheal mice with kidney-yang deficiency syndrome. **Notes**: (**A**) Relative abundance at the phylum level; (**B**) Relative abundance at the genus level; (**C–F**) Dominant genera in the small intestinal mucosa of each group. *p<0.05; **p<0.01. CC: Normal group; NR: Natural recovery group; CB: Sodium Butyrate group; CS: SSP group; CR: 100 mg/kg sodium butyrate + 50% SSP group.

not statistically significant ($p > 0.05$) (Figure 7D). Sodium butyrate was observed to restore the relative abundance of *Lactobacillus* in the small intestinal mucosa of diarrheal mice with kidney-yang deficiency syndrome (Figure 7E). Compared with that in the normal group, the relative abundance of *Corynebacterium* significantly increased in the natural recovery group ($p < 0.05$). This abundance decreased across all treatment groups, with the 100 mg/kg sodium butyrate + 50% SSP combination group showing a highly significant difference in *Corynebacterium* relative abundance compared with the natural recovery group ($p < 0.01$) (Figure 7F).

Effects on the Characteristic Microbiota of the Small Intestinal Mucosa in Mice

LEfSe analysis was performed to identify significantly different microbial taxa among the experimental groups, with a score threshold set at >2. As shown in Figure 8A, LEfSe analysis between the normal group and the natural recovery group revealed that *ZJ304, Desulfovibrio_R, Nanosyncoccus*, and *Parvimonas* were significantly enriched in the normal group, whereas *Corynebacterium, Mammaliicoccus, Anaerococcus, Acinetobacter, Kurthia, Aerococcus*, and *Facklamia_A* were significantly enriched in the natural recovery group. As shown in Figure 8B, LEfSe analysis between the natural recovery group and the SSP group revealed that *Berryella* and *Dialister* were the enriched characteristic genera in the SSP group, whereas *Corynebacterium, Mammaliicoccus, Anaerococcus*, and *UBA7173* (along with 7 other genera) were the enriched characteristic genera in the natural recovery group. As shown in Figure 8C, LEfSe analysis between the natural recovery group and the sodium butyrate group revealed that *Diaphorobacter_A* was the enriched characteristic genus in the sodium butyrate group, whereas *UBA7173, CAG_873, Duncaniella, Paramuribaculum*, and *Adlercreutzia* were the enriched characteristic genera in the natural recovery group. As shown in Figure 8D, LEfSe analysis between the natural recovery group and the 100 mg/kg sodium butyrate + 50% SSP group revealed that *Dialister, Helicobacter_A*, and *Parvimonas* were the enriched characteristic genera in the 100 mg/kg sodium butyrate + 50% SSP group, whereas *Corynebacterium, Staphylococcus, Mammaliicoccus, Escherichia*, and 6 other genera were the enriched characteristic genera in the natural recovery group.

To further analyse the effects of sodium butyrate, SSP, and their combination on the intestinal mucosal microbiota of mice, we established a random forest model to identify the top 10 characteristic genera in each experimental group

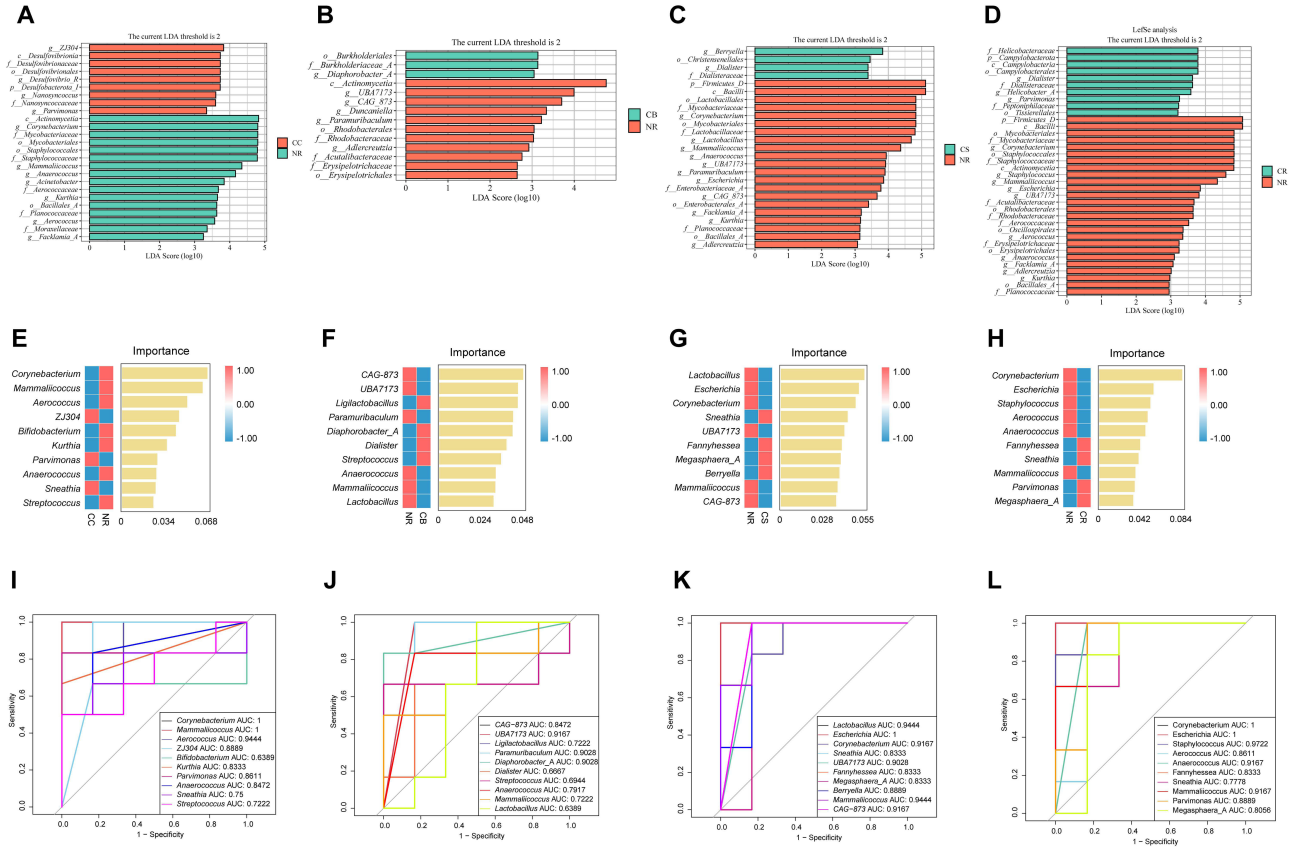

Figure 8 Analysis of characteristic genera in the small intestinal mucosa of mice.
Notes: (**A–D**) Genus-level LDA analysis. (**E–H**) Genus-level random forest analysis. (**I**) Genus-level ROC analysis (CC vs NR). (**J**) Genus-level ROC analysis (NR vs CB). (**K**) Genus-level ROC analysis (NR vs CS). (**L**) Genus-level ROC analysis (NR vs CR). CC: Normal group; NR: Natural recovery group; CB: Sodium Butyrate group; CS: SSP group; CR: 100 mg/kg sodium butyrate + 50% SSP group.

(Figure 8E–H). ROC analysis was subsequently performed on the selected characteristic genera, and genera with an AUC > 0.8 were used as the standard to verify their accuracy in diagnosing intergroup differences, thereby determining their diagnostic capability (Figure 8I–L). In the ROC analysis between the normal and natural recovery groups, the genera with an AUC > 0.8 were *Corynebacterium* (AUC = 1), *Mammaliicoccus* (AUC = 1), *Aerococcus* (AUC = 0.9444), *ZJ304* (AUC = 0.8889), *Kurthia* (AUC = 0.8333), *Parvimonas* (AUC = 0.8611), and *Anaerococcus* (AUC = 0.8472). In the ROC analysis between the natural recovery group and the SSP group, the genera with an AUC > 0.8 were *Lactobacillus* (AUC = 0.9444), *Escherichia* (AUC = 1), *Corynebacterium* (AUC = 0.9167), *Sneathia* (AUC = 0.8333), *UBA7173* (AUC = 0.9028), *Fannyhessea* (AUC = 0.8333), *Megasphaera_A* (AUC = 0.8333), *Berryella* (AUC = 0.8889), *Mammaliicoccus* (AUC = 0.9444), and *CAG−873* (AUC = 0.9167). In the ROC analysis between the natural recovery group and the sodium butyrate group, the genera with an AUC > 0.8 were *CAG−873* (AUC = 0.8472), *UBA7173* (AUC = 0.9167), *Paramuribaculum* (AUC = 0.9028), and *Diaphorobacter_A* (AUC = 0.9028). In the ROC analysis between the natural recovery and 100 mg/kg sodium butyrate + 50% SSP groups, the genera with an AUC > 0.8 were *Corynebacterium* (AUC = 1), *Escherichia* (AUC = 1), *Staphylococcus* (AUC = 0.9722), *Aerococcus* (AUC = 0.8611), *Anaerococcus* (AUC = 0.9167), *Fannyhessea* (AUC = 0.8333), *Mammaliicoccus* (AUC = 0.9167), *Parvimonas* (AUC = 0.8889), and *Megasphaera_A* (AUC = 0.8056). These findings indicate that the above genera exhibit differences in abundance and diagnostic efficacy. The combination of LEfSe, random forest, and ROC curve analyses identified *Corynebacterium* and *Mammaliicoccus* as key members of the intestinal mucosal microbiota in diarrhea patients with

https://doi.org/10.2147/JIR.S518370

kidney-yang deficiency syndrome. These genera have diagnostic for the syndrome and can be used to evaluate the therapeutic effects of sodium butyrate, SSP, and their combination.

Correlation Analysis of Sodium Butyrate, Sishen Pill, and Their Combinations in the Treatment of Diarrhea with Kidney-Yang Deficiency Syndrome

Random forest analysis was applied to explore the relationships between the small intestinal microbiota and inflammatory or mucosal protective factors in the treatment of diarrhea in patients with kidney-yang deficiency syndrome via the use of sodium butyrate, SSP, or their combination. The top 10 genus-level characteristic bacteria in each experimental group that met the ROC analysis criterion (AUC > 0.8) were subjected to Spearman correlation analysis with the IL-6, TNF-α, MUC2, and sIgA levels in the mice. Figure 9A shows that in the genus-level characteristic bacterial analysis

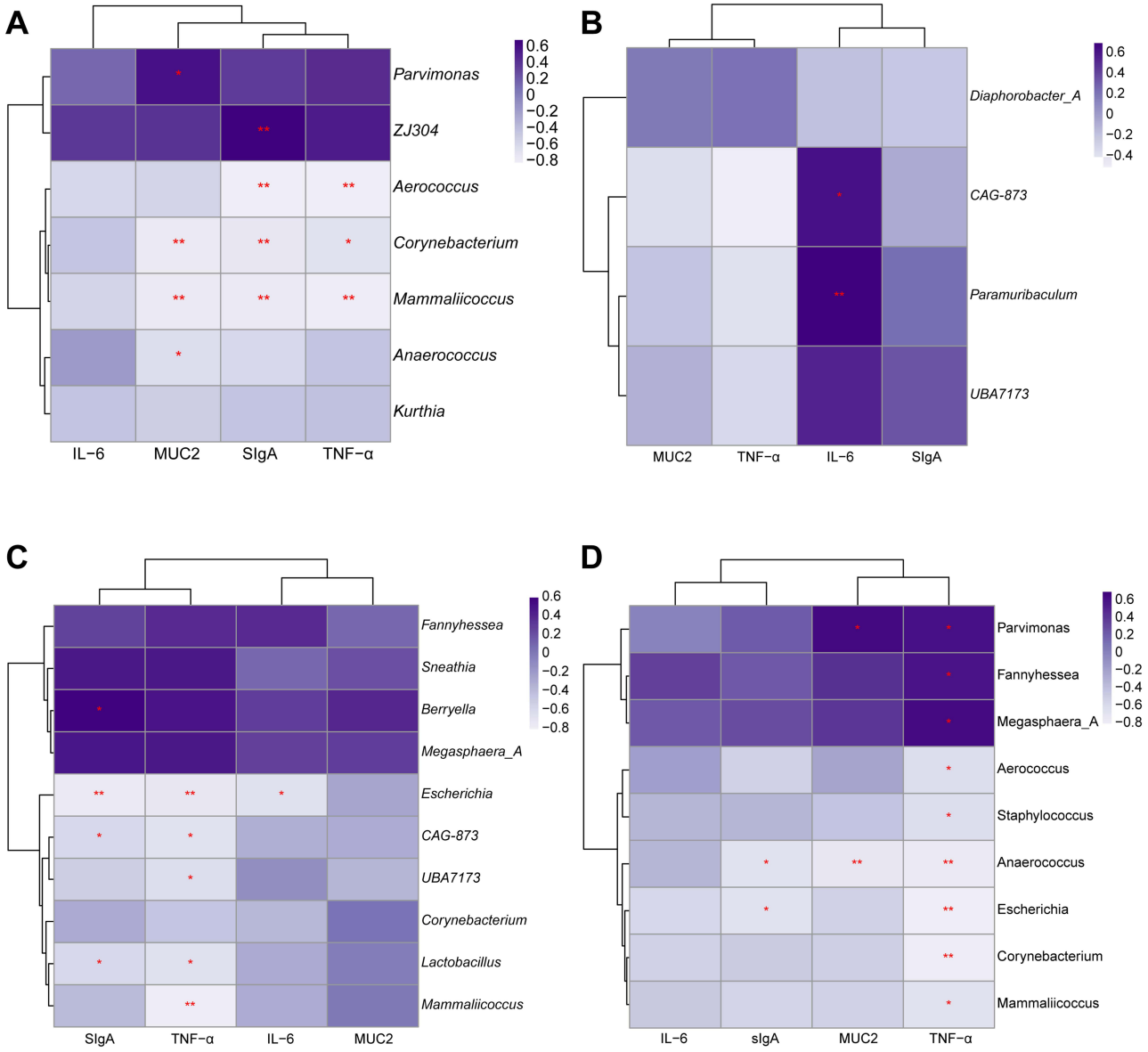

Figure 9 Correlation analysis between genus-level characteristic bacteria and serum TNF-α and IL-6 levels and colonic sIgA and MUC2 levels.
Notes: (**A**) CC vs NR; (**B**) NR vs CB; (**C**) NR vs CS; (**D**) NR vs CR. CC: Normal group; NR: Natural recovery group; CB: Sodium Butyrate group; CS: SSP group; CR: 100 mg/kg sodium butyrate + 50% SSP group. *p<0.05; **p<0.01; ***p<0.001. CC: Normal group; NR: Natural recovery group; CB: Sodium Butyrate group; CS: SSP group; CR: 100 mg/kg sodium butyrate + 50% SSP group.

between the normal group and the natural recovery group, *Anaerococcus* ($p < 0.05$), *Mammaliicoccus* ($p < 0.01$), and *Corynebacterium* ($p < 0.01$) were significantly negatively correlated with MUC2, whereas *Parvimonas* ($p < 0.05$) was significantly positively correlated with MUC2. *Mammaliicoccus* ($p < 0.01$), *Corynebacterium* ($p < 0.01$), and *Aerococcus* ($p < 0.01$) were significantly negatively correlated with sIgA, whereas *ZJ304* ($p < 0.01$) was significantly positively correlated with sIgA. Additionally, *Mammaliicoccus* ($p < 0.01$), *Corynebacterium* ($p < 0.05$), and *Aerococcus* ($p < 0.01$) were significantly negatively correlated with TNF-α. Figure 9B shows that in the analysis of characteristic bacteria at the genus level between the natural recovery group and the SSP group, *Lactobacillus* ($p < 0.05$), *CAG−873* ($p < 0.05$), and *Escherichia* ($p < 0.01$) were significantly negatively correlated with sIgA, whereas *Berryella* ($p < 0.05$) was significantly positively correlated with sIgA. *Mammaliicoccus* ($p < 0.01$), *Lactobacillus* ($p < 0.05$), *UBA7173* ($p < 0.05$), *CAG−873* ($p < 0.05$), and *Escherichia* ($p < 0.01$) were significantly negatively correlated with TNF-α, and *Escherichia* ($p < 0.05$) was significantly negatively correlated with IL-6. Figure 9C shows that in the genus-level analysis of characteristic bacteria between the natural recovery group and the sodium butyrate group, *Paramuribaculum* ($p < 0.01$) and *CAG−873* ($p < 0.05$) were significantly positively correlated with IL-6. Figure 9D shows that in the genus-level analysis of characteristic bacteria between the natural recovery group and the 100 mg/kg butyrate sodium + 50% SSP group, *Escherichia* ($p < 0.05$) and *Anaerococcus* ($p < 0.05$) were significantly negatively correlated with sIgA; *Anaerococcus* ($p < 0.01$) was significantly negatively correlated with MUC2, whereas *Parvimonas* ($p < 0.05$) was significantly positively correlated with MUC2; *Parvimonas* ($p < 0.05$), *Fannyhessea* ($p < 0.05$), and *Megasphaera_A* ($p < 0.05$) were significantly positively correlated with TNF-α, whereas *Aerococcus* ($p < 0.05$), *Staphylococcus* ($p < 0.05$), *Anaerococcus* ($p < 0.01$), *Escherichia* ($p < 0.01$), *Corynebacterium* ($p < 0.01$), and *Mammaliicoccus* ($p < 0.05$) were significantly negatively correlated with TNF-α.

Effects of Sodium Butyrate, SSP, and Their Combinations on the Function of the Mouse Small Intestinal Mucosal Microbiome

We used PICRUSt2, which is based on the KEGG database, to predict and analyse microbial metabolic pathways to evaluate changes in the metabolism and function of the small intestinal mucosal microbiome in diarrheal kidney-yang deficiency syndrome mice under different treatments. The functional analysis of the intestinal mucosal microbiome can generally be divided into six major categories, with metabolic functions having the highest abundance among all subfunctional categories (Figure 10A). Among them, metabolic pathways greater than two times the median were selected, mainly including 10 categories such as amino acid metabolism, carbohydrate metabolism, energy metabolism, and metabolism of cofactors and vitamins (Figure 10B). Further statistical analysis of the selected third-level metabolic pathways (Figure 10C) revealed that, compared with that in the normal group, the secondary bile acid biosynthesis pathway was significantly reduced in diarrheal mice with kidney-yang deficiency syndrome ($p<0.01$), and a certain degree of recovery was observed in the sodium butyrate group and the 100 mg/kg sodium butyrate + 50% SSP group, with the sodium butyrate group recovering to levels not significantly different from those of the normal group ($p>0.05$). The biosynthesis of ansamycins pathway was also significantly reduced in diarrheal mice with kidney-yang deficiency syndrome ($p<0.01$), but after treatment, the SSP group, sodium butyrate group, and 100 mg/kg sodium butyrate + 50% SSP group presented varying degrees of recovery, with the SSP group and the 100 mg/kg sodium butyrate + 50% SSP group showing significant increases compared with the natural recovery group ($p<0.01$). The biosynthesis of vancomycin group antibiotics pathway showed a decreasing trend in the natural recovery group compared to the normal group, with increases observed in the SSP, sodium butyrate, and 100mg/kg sodium butyrate + 50% SSP groups, but no significant differences between groups ($p>0.05$). The fatty acid biosynthesis pathway was increased in diarrheal mice with kidney-yang deficiency syndrome and was restored in the 100 mg/kg sodium butyrate + 50% SSP group, but no significant differences were found between the groups ($p>0.05$). These findings indicate that diarrhea in kidney-yang deficiency syndrome leads to an overall decline in metabolic functions in mice and that both sodium butyrate and SSP play an active role in restoring these metabolic functions, with the combination of both showing some advantages in restoring metabolic function.

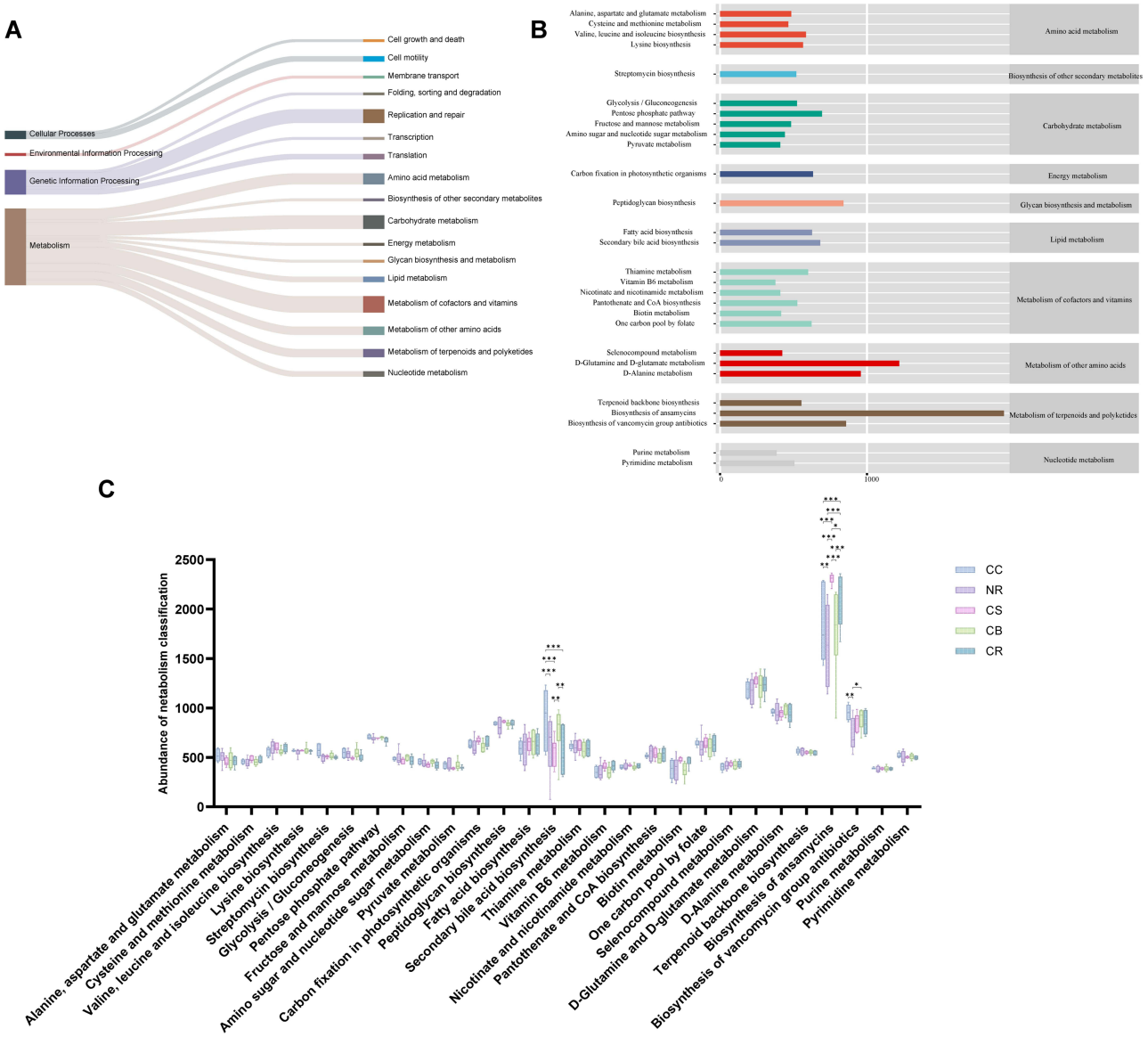

Figure 10 PICRUSt2 prediction and microbial-related metabolic pathway information on the basis of the KEGG database.
Notes: (**A**) KEGG functional pathways; (**B**) Histogram of metabolic pathway abundance; (**C**) Comparison of metabolic functions between groups (tertiary level). *p<0.05; **p<0.01; ***p<0.001. CC: Normal group; NR: Natural recovery group; CB: Sodium Butyrate group; CS: SSP group; CR: 100 mg/kg sodium butyrate + 50% SSP group.

Discussion

The gastrointestinal tract is colonized by a vast array of microorganisms, including bacteria, fungi, and viruses, collectively referred to as the intestinal microbiota, which is considered the "second genome" of the human body.[23] This microbiota begins to develop at birth and stabilizes over time as an individual ages. Intestinal homeostasis primarily involves dynamic interactions among the host, the intestinal microbiota, nutrients, and metabolic products. This balance is crucial not only for food digestion and energy metabolism but also for influencing the host's immune response and maintaining overall health.[24] Any imbalance in the intestinal microbiota can lead to disease development. Research has shown that, in diarrheal mice with kidney-yang deficiency syndrome, the richness and diversity of the intestinal microbiota are higher than those in normal mice, and the microbial community structure becomes more dispersed.[25] This study used bioinformatics techniques to analyse changes in the small intestinal mucosal microbiota of diarrheal mice with kidney-yang deficiency syndrome following different interventions. Our study revealed that the composition of the small intestinal mucosal microbiota changed across the diarrhea model and various treatment groups. PCoA revealed differences between the microbiota of diarrheal mice with kidney-yang deficiency

syndrome and those of normal mice. After treatment with sodium butyrate and the combination therapy, the samples clustered more closely together, with reduced inter-group variability. Furthermore, there was a significant difference in the intestinal microbiota structure between the mice in the combined treatment group and those in the naturally recovered mice, which was also confirmed by the PERMANOVA test results. Suggesting that the combination of SSP and sodium butyrate can effectively restore the intestinal microbiota homeostasis in diarrheal mice with kidney-yang deficiency syndrome. Although alpha diversity indices such as Chao1 and Shannon showed no significant differences between groups, the observed changes in beta diversity indicate that the microbial community structure underwent notable compositional shifts. This discrepancy suggests that while the overall richness and evenness of the gut microbiota were preserved, the relative abundance of specific taxa was significantly altered by the treatments. The functional or pathological outcomes can be more closely associated with taxonomic composition rather than total diversity. Therefore, the therapeutic effects observed in the sodium butyrate and Sishen Pill treatment groups may result from targeted modulation of key microbial taxa rather than broad changes in microbial diversity.

Interventions with sodium butyrate and SSP also altered the relative abundances of the dominant phyla and genera in the small intestinal mucosa of diarrheal mice with kidney-yang deficiency syndrome. Compared with those of the normal group, the relative abundances of *Dwaynesavagella, Megasphaera_A*, and *Lactobacillus* tended to decrease in the small intestinal mucosa of diarrheal mice with kidney-yang deficiency syndrome. However, following treatment, the relative abundances of *Dwaynesavagella* and *Megasphaera_A* increased across all the intervention groups. Notably, sodium butyrate had a significant restorative effect on the relative abundances of *Dwaynesavagella, Megasphaera_A*, and *Lactobacillus*. Furthermore, combination therapy with sodium butyrate and SSP exhibited a distinct advantage in restoring the relative abundance of *Megasphaera_A*. Notably, the relative abundance of *Corynebacterium* significantly increased in diarrheal mice with kidney-yang deficiency syndrome but decreased after treatment. Among the treatment groups, the combination of sodium butyrate and SSP had a pronounced ability to control the relative abundance of *Corynebacterium. Dwaynesavagella* (*Candidatus Savagella*), also referred to as Segmented Filamentous Bacteria (SFB), are strict anaerobes that attach to the intestinal epithelium of animal hosts and tightly bind to the absorptive intestinal epithelial surface. It can stimulate the maturation of host Th17 and IgA responses and competitively inhibit other intestinal pathogenic microorganisms, thereby controlling the occurrence of inflammatory responses. SFB plays a critical role in establishing and maintaining a healthy intestine and is beneficial in controlling and treating diseases such as colitis.[26] *Megasphaera_A* is closely linked to the occurrence of diarrhoeal diseases. Studies have shown that in children with acute diarrhea caused by the *Cryptosporidium* genus, the abundance of *Megasphaera* is significantly reduced.[27] Moreover, in predicting subclinical (non-diarrheal) diseases, the abundance of *Megasphaera* can serve as an important indicator. *Corynebacterium*, a gram-positive bacillus, typically proliferates on mucosal surfaces and secretes exotoxins, causing localized inflammation. In immunocompromised hosts, it can become pathogenic and is considered an opportunistic pathogen. Research on the intestinal microbiota of colorectal cancer (CRC) patients has revealed a close association between *Corynebacterium* and CRC, with a notably higher relative abundance in invasive cancer groups. This finding aligns with the observed increase in *Corynebacterium* in the natural recovery group in this study.[28]

When biological tissues are stimulated by pathogenic infections or other factors, an inflammatory response is triggered. Inflammation is akin to a double-edged sword, while excessive inflammation can have adverse effects on the body, under normal circumstances, it plays an essential role in bolstering the body's defense mechanisms. Inflammatory factors, which include various cytokines involved in the inflammatory response, activate the body's immune system and influence the progression of diseases. TNF-α is a critical inflammatory mediator that can activate neutrophils and lymphocytes, regulate the metabolic activity of other tissues, and thereby facilitate disease recovery.[29] Studies have shown that pharmacological inhibition of TNF-α effectively controls acute inflammation in rats with oral ulcers but significantly delays wound healing, thereby slowing the recovery process.[30] Similarly, IL-6, another common inflammatory cytokine, induces B-cell differentiation and antibody production; promotes T-cell activation, proliferation, and differentiation; and participates in immune responses.[31–33] Research on psoriasis treatment has revealed that anti-IL-6 therapy may trigger compensatory proinflammatory cytokine production, exacerbating inflammation in psoriasis patients.[34] In this study, naturally recovering mice with diarrhea induced by kidney-yang deficiency syndrome presented reduced TNF-α and IL-6 levels. However, after interventions with sodium butyrate, SSP, or their combination, the levels of these cytokines increased to some extent. This phenomenon might indicate suppressed immune function in diarrheal mice with kidney-yang deficiency syndrome, with SSP potentially enhancing kidney-yang and immune activity. At the same time, we observed that TNF-α levels were lower in the natural recovery group but increased with treatment.

However, IL-6 did not show significant changes. This may reflect pathway-specific regulatory effects of the treatment. TNF-α as a key pro-inflammatory cytokine primarily produced by activated macrophages and plays an early and central role in initiating intestinal inflammation., whereas IL-6 is not only involved in inflammation but also in immune regulation. Its expression can be influenced by a broader range of stimuli and feedback mechanisms. The observed discrepancy suggests that sodium butyrate and Sishen Pill may selectively influence TNF-α–mediated acute inflammation without significantly altering IL-6–dependent compensatory pathways. Moreover, sIgA and MUC2 play vital roles in protecting mucosal surfaces from pathogenic invasion and maintaining microbial balance.[35,36] In this study, interventions with both sodium butyrate and SSP increased sIgA and MUC2 levels, facilitating the repair of intestinal damage in diarrheal mice with kidney-yang deficiency syndrome. The combination treatment had a more pronounced effect. *Mammaliicoccus*, a phylogenetically related gram-positive coccus, is part of many commensal microbiota. Studies have shown that it can cause infectious diseases in animals.[37,38] LEfSe analysis identified microbial biomarkers in each group. In the natural recovery group, *Corynebacterium* and *Mammaliicoccus* was significantly negatively correlated with both sIgA and MUC2 levels. This suggests that these genera may play a role in disrupting intestinal barrier function. Although the precise mechanisms remain to be fully elucidated, previous studies have indicated that certain pathogenic species within these genera may impair mucosal integrity by secreting exotoxins or damaging mucus structures, thereby weakening MUC2 function or inhibiting the normal expression of sIgA. The increased abundance of *Corynebacterium* and *Mammaliicoccus* may also contribute to intestinal dysbiosis, which could reduce the levels of beneficial bacteria essential for the survival and function of intestinal epithelial cells.[39] Moreover, MUC2 serves as a binding platform for sIgA, facilitating the neutralization of pathogens; thus, impairment of MUC2 may indirectly compromise the protective role of sIgA as well.[40] However, further experimental validation is needed to confirm their specific pathogenic roles. Among the characteristic genera of the combination group, *Parvimonas* was significantly positively correlated with sIgA and MUC2 levels, which is consistent with the observed changes in these biomarkers across groups.

The renal are often damaged due to inflammatory cell infiltration and other factors, whereas the intestines may experience functional impairment caused by atrophy or injury to mucosal or villous structures.[41,42] Previous studies have shown that diarrhea with kidney-yang deficiency syndrome leads to varying degrees of damage to the intestinal and renal tissues of mice, which can be alleviated following treatment with SSP.[43,44] Additionally, sodium butyrate plays a significant role in restoring intestinal structure and regulating intestinal function.[45] The findings revealed that the SSP group exhibited a pronounced effect on restoring intestinal villous structures, whereas sodium butyrate had an advantage in influencing crypt depth. Crypt depth is a key histological indicator of intestinal health, as it reflects the regenerative capacity of the intestinal epithelium. Intestinal crypts are the sites of epithelial stem cell proliferation, which supports the continuous renewal and migration of epithelial cells toward the villus surface. Appropriate crypt architecture is essential for maintaining epithelial integrity, nutrient absorption, and mucosal barrier function. Abnormal increases in crypt depth may indicate epithelial hyperplasia or disordered regeneration, often associated with chronic inflammation or injury. Therefore, restoration of normal crypt architecture is considered an important marker of mucosal recovery and intestinal homeostasis.[46,47] The combination of sodium butyrate and SSP has a significant synergistic effect on restoring villous length, reducing crypt depth, and mitigating renal inflammatory infiltration. Furthermore, during the modelling process, the use of adenine was found to reduce the liver index in mice,[48] which aligns with the trends observed in this study. Notably, combined treatment with sodium butyrate and SSP effectively restored the liver index in diarrheal mice with kidney-yang deficiency syndrome. These results suggest that the combined use of sodium butyrate and SSP may serve as a novel approach for treating diarrhea in patients with kidney-yang deficiency syndrome. Metabolic pathway analysis revealed an overall decline in metabolic functions in these mice, while the effectiveness of the combined therapy may be attributed to enhanced pathways such as secondary bile acid biosynthesis, biosynthesis of ansamycins, and biosynthesis of vancomycin group antibiotics, as well as a reduction in the fatty acid biosynthesis pathway. Future research could focus on these metabolic pathways to further elucidate the mechanisms underlying this combined therapy or explore new treatment strategies for this condition. Although PICRUSt2-based functional predictions provided insights into potential shifts in microbial metabolic activity, it is important to acknowledge that such predictions are inferential and based on 16S rRNA gene sequences rather than direct metagenomic or metatranscriptomic data. Therefore, the predicted pathways should be interpreted with caution. Future studies incorporating shotgun metagenomics or metabolomics are warranted to validate the functional consequences of microbial community changes observed in this model.

TCMs are primarily administered orally, making the gastrointestinal tract the primary site of interaction. TCMs exert their therapeutic effects by influencing the structure of the intestinal microbiota.[49] Conversely, the intestinal microbiota can metabolize and utilize compounds from TCMs, creating a mutually reinforcing relationship.[50,51] In addition to regulating the structure of the intestinal microbiota, TCMs also impact the production of their metabolites. Among microbial metabolites, SCFAs have been extensively studied. SCFAs, including acetate, propionate, and butyrate, play vital roles as energy sources and in maintaining intestinal homeostasis. The abundance of SCFAs in the body is closely linked to TCMs. For example, SSP influences the "L. johnsonii–propionic acid" pathway to promote the production of propionic acid, butyric acid, isobutyric acid, and isovaleric acid in the intestine, thereby suppressing intestinal inflammation.[15] Qiwei Baizhu powder has been shown to restore acetate and butyrate levels depleted by antibiotics, enhancing the ability of the intestine to inhibit pathogenic bacteria.[52] Additionally, research on *Forsythiae Fructus* revealed that its active compound forsythiaside A significantly increases the levels of acetate, propionate, isobutyric acid, butyrate, and hexanoic acid, thereby protecting the liver.[53] In conclusion, the interaction between TCMs and the intestinal microbiota is crucial for treating intestinal microbiota imbalances and gastrointestinal diseases involving mucosal damage. The effect of TCMs on SCFAs highlights their therapeutic potential in managing diarrhea associated with kidney-yang deficiency syndrome. These findings suggest that supplementing SCFAs during TCM treatment may further enhance recovery and promote overall health maintenance.

Conclusion

Building on previous studies, this study successfully established a mouse model of diarrhea with kidney-yang deficiency syndrome and explored the effects of SSP, sodium butyrate, and their combination on this condition. The findings revealed that sodium butyrate, SSP, and their combination effectively alleviated symptoms of diarrhea in patients with kidney-yang deficiency syndrome to varying degrees. These treatments induced changes in the structure and function of the small intestinal mucosal microbiota, restored immune function, and protected the intestinal mucosa from pathogen-induced damage. Overall, the combination of sodium butyrate and SSP had superior therapeutic effects. It significantly reduced the abundance of *Corynebacterium* in diarrheal mice with kidney-yang deficiency syndrome, increased the levels of sIgA and MUC2, and promoted the repair of damaged intestinal and renal tissues. However, considering the complexity of the pathogenesis of diarrhea in patients with kidney-yang deficiency syndrome and the diverse composition of traditional Chinese medicine, further validation of this approach is necessary. Meanwhile, due to the lack of a comprehensive dose–response analysis, the observed efficacy should not be interpreted as the definitive optimal ratio. Future studies should focus on identifying the most effective dosing strategy, elucidating the synergistic mechanism of sodium butyrate and SSP at the molecular and microbial levels, and validating the findings in broader experimental or clinical contexts. Therefore, future experiments should employ multiple approaches to investigate the mechanisms underlying the therapeutic effects of sodium butyrate and SSP on diarrhea in patients with kidney-yang deficiency syndrome.

Abbreviations

SSP, Sishen Pill; TCM, traditional Chinese medicine; TMAO, Trimethylamine-N-oxide; SCFAs, Short-chain fatty acids; ELISA, enzyme-linked immunosorbent assay; ASVs, amplicon sequence variants; PCoA, principal coordinate analysis; LEfSe, linear discriminant analysis effect size.

Data Sharing Statement

The datasets presented in this study can be found in online repositories. The names of the repository/repositories and accession number(s) can be found below: https://www.ncbi.nlm.nih.gov/, PRJNA1121031.

Ethics Approval and Consent to Participate

The animal experiments were approved by the Animal Ethics and Welfare Committee of Hunan University of Traditional Chinese Medicine, and complied with the requirements of animal ethics (Ethics No. HNUCM21-2403-43).

Acknowledgments

We appreciate all the help for this work.

Funding

This research is financially supported by the Key Scientific Research Project of Hunan Provincial Education Department (24A0278).

Disclosure

The authors report no conflicts of interest in this work.

References

1. Li X, Tan Z. Modern biological connotation of diarrhea with kidney-Yang deficiency syndrome. *World China J Digestol*. 2022;30:119–127. doi:10.11569/wcjd.v30.i3.119
2. Zhang P, Jin W, Lyu Z, Lyu X, Li L. Study on the mechanism of gut microbiota in the pathogenetic interaction between depression and Parkinson 's disease. *Brain Res Bull*. 2024;215:111001. doi:10.1016/j.brainresbull.2024.111001
3. Qi X, Yun C, Pang Y, Qiao J. The impact of the gut microbiota on the reproductive and metabolic endocrine system. *Gut Microbes*. 2021;13:1–21. doi:10.1080/19490976.2021.1894070
4. Chénard T, Prévost K, Dubé J, Massé E. Immune system modulations by products of the gut microbiota. *Vaccines*. 2020;8:461. doi:10.3390/vaccines8030461
5. Yu D, Xie S, Guo M, et al. External damp environment aggravates diarrhea in spleen deficiency and dampness syndrome in mice: involvement of small intestinal contents microbiota, energy metabolism, gastrointestinal and fluid functions. *Front Cell Infect Microbiol*. 2024;14:1495311. doi:10.3389/fcimb.2024.1495311
6. Xie S, Deng N, Fang L, Shen J, Tan Z, Cai Y. TMAO is involved in kidney-yang deficiency syndrome diarrhea by mediating the "gut-kidney axis". *Heliyon*. 2024;10:e35461. doi:10.1016/j.heliyon.2024.e35461
7. Wang K, Li G, Yang Z, et al. Compound Chinese medicine (F1) improves spleen deficiency diarrhea by protecting the intestinal mucosa and regulating the intestinal flora. *Front Microbiol*. 2023;14:1292082. doi:10.3389/fmicb.2023.1292082
8. Li XY, Wang ZM, Yao XH, et al. Research progress on pharmacological effects and clinical application of sishen pill. *J Liaoning Univ Traditional Chin Med*. 2021;23:122–126.
9. Zhang B, Cheng Y, Jian Q, et al. Sishen Pill and its active phytochemicals in treating inflammatory bowel disease and colon cancer: an overview. *Front Pharmacol*. 2024;15:1375585. doi:10.3389/fphar.2024.1375585
10. Li SQ, Hu YL, Su CX, et al. Sishenwan ameliorates visceral sensitivity in rat model of diarrhea-predominant irritable bowel syndrome (Spleen-kidney Yang Deficiency)by regulating p38 MAPK/JNK/TRPV1 pathway. *Chin J Exp Tradit Med Formulae*. 2024;30:10–18.
11. Huang J, Zhong Y, Cheng N, et al. Sishen pills inhibit inflammatory dendritic cell differentiation via miR-505-3p mediated E-cadherin down-regulation in ulcerative colitis. *Phytomedicine*. 2024;135:156035. doi:10.1016/j.phymed.2024.156035
12. Xie S, Fang L, Deng N, Shen J, Tan Z, Peng X. Targeting the gut-kidney axis in diarrhea with kidney-yang deficiency syndrome: the role of sishen pills in regulating TMAO-mediated inflammatory response. *Med Sci Monit*. 2024;30:e944185. doi:10.12659/MSM.944185
13. Du YW, Li J, Wang YL, Zou DW. Study of different effect of fructus schisandrae chinensis powder and sishen pill on Wistar rats of diarrhea of the contents of sIgA and IL-2. *Chin Arch Tradit Chin Med*. 2009;27:2189–2191.
14. Zhao Y, Zhan J, Sun C, et al. Sishen Wan enhances intestinal barrier function via regulating endoplasmic reticulum stress to improve mice with diarrheal irritable bowel syndrome. *Phytomedicine*. 2024;129:155541. doi:10.1016/j.phymed.2024.155541
15. Li X, Qiao B, Wu Y, Deng N, Yuan J, Tan Z. Sishen pill inhibits intestinal inflammation in diarrhea mice via regulating kidney-intestinal bacteria-metabolic pathway. *Front Pharmacol*. 2024;15:1360589. doi:10.3389/fphar.2024.1360589
16. Di JX, Guo MF, Xiao NQ, Tan ZJ. Research progress of intestinal butyric acid. *Chin J Infect Control*. 2024;23:1192–1198.
17. Luo D, Li J, Xing T, Zhang L, Gao F. Combined effects of xylo-oligosaccharides and coated sodium butyrate on growth performance, immune function, and intestinal physical barrier function of broilers. *Anim Sci J*. 2021;92:e13545. doi:10.1111/asj.13545
18. Li C, Chen J, Zhao M, et al. Effect of sodium butyrate on slaughter performance, serum indexes and intestinal barrier of rabbits. *J Anim Physiol Anim Nutr*. 2022;106:156–166. doi:10.1111/jpn.13571
19. Xu HM. *The Role and Mechanism of Butyric Acid in the Treatment of Ulcerative Colitis by Fecal Microbiota Transplantation* [dissertation]. China: South China University of Technology; 2023.
20. Guo KX, Tan ZJ, Xie MZ, She Y, Wang XH. The synergic effect of ultra-micro powder Qiweibaizhusan combined with yeast on dysbacteriotic diarrhea mice. *Chin J Appl Environ Biol*. 2015;21:61–67.
21. Li XY, Zhu JY, Wu Y, Liu YW, Hui HY, Tan ZJ. Model building and validation of diarrhea mice with kidney-yang depletion syndrome. *J Tradit Chin Med*. 2022;63:1368–1373.
22. Lewis SM, Williams A, Eisenbarth SC. Structure and function of the immune system in the spleen. *Sci Immunol*. 2019;4:eaau6085. doi:10.1126/sciimmunol.aau6085
23. Behera J, Ison J, Tyagi SC, Tyagi N. The role of gut microbiota in bone homeostasis. *Bone*. 2020;135:115317. doi:10.1016/j.bone.2020.115317
24. Wang J, Zhu N, Su X, Gao Y, Yang R. Gut-microbiota-derived metabolites maintain gut and systemic immune homeostasis. *Cells*. 2023;12:793. doi:10.3390/cells12050793
25. Zhu J, Li X, Deng N, Peng X, Tan Z. Diarrhea with deficiency kidney-yang syndrome caused by adenine combined with folium senna was associated with gut mucosal microbiota. *Front Microbiol*. 2022;13:1007609. doi:10.3389/fmicb.2022.1007609
26. Hedblom GA, Reiland HA, Sylte MJ, Johnson TJ, Baumler DJ. Segmented filamentous bacteria - metabolism meets immunity. *Front Microbiol*. 2018;9:1991. doi:10.3389/fmicb.2018.01991
27. Carey MA, Medlock GL, Alam M, et al. Megasphaera in the stool microbiota is negatively associated with diarrheal cryptosporidiosis. *Clin Infect Dis*. 2021;73:e1242–1242e1251. doi:10.1093/cid/ciab207

28. Zorron Cheng Tao Pu L, Yamamoto K, Honda T, et al. Microbiota profile is different for early and invasive colorectal cancer and is consistent throughout the colon. *J Gastroenterol Hepatol*. 2020;35:433–437. doi:10.1111/jgh.14868
29. van der Houwen T, van Laar J. Behçet's disease, and the role of TNF-α and TNF-α blockers. *Int J Mol Sci*. 2020;21:3072. doi:10.3390/ijms21093072
30. Freitas MO, Fonseca A, de Aguiar MT, et al. Tumor necrosis factor alpha (TNF-α) blockage reduces acute inflammation and delayed wound healing in oral ulcer of rats. *Inflammopharmacology*. 2022;30:1781–1798. doi:10.1007/s10787-022-01046-3
31. Kerkis I, Silva da SÁP, Araldi RP, Silva ÁPD. The impact of interleukin-6 (IL-6) and mesenchymal stem cell-derived IL-6 on neurological conditions. *Front Immunol*. 2024;15:1400533. doi:10.3389/fimmu.2024.1400533
32. Hirano T. IL-6 in inflammation, autoimmunity and cancer. *Int Immunol*. 2021;33:127–148. doi:10.1093/intimm/dxaa078
33. Jones BE, Maerz MD, Buckner JH. IL-6: a cytokine at the crossroads of autoimmunity. *Curr Opin Immunol*. 2018;55:9–14. doi:10.1016/j.coi.2018.09.002
34. Blauvelt A. IL-6 differs from TNF-α: unpredicted clinical effects caused by IL-6 blockade in psoriasis. *J Invest Dermatol*. 2017;137:541–542. doi:10.1016/j.jid.2016.11.022
35. Di Sabatino A, Santacroce G, Rossi CM, Broglio G, Lenti MV. Role of mucosal immunity and epithelial-vascular barrier in modulating gut homeostasis. *Intern Emerg Med*. 2023;18:1635–1646. doi:10.1007/s11739-023-03329-1
36. Liu Y, Yu X, Zhao J, Zhang H, Zhai Q, Chen W. The role of MUC2 mucin in intestinal homeostasis and the impact of dietary components on MUC2 expression. *Int J Biol Macromol*. 2020;164:884–891. doi:10.1016/j.ijbiomac.2020.07.191
37. Schwendener S, Perreten V. The bla and mec families of β-lactam resistance genes in the genera macrococcus, Mammaliicoccus and staphylococcus: an in-depth analysis with emphasis on macrococcus. *J Antimicrob Chemother*. 2022;77:1796–1827. doi:10.1093/jac/dkac107
38. Dhaouadi S, Bouchami O, Soufi L, et al. Frequent dissemination and carriage of an SCCmec-mecC hybrid in methicillin-resistant Mammaliicoccus sciuri in farm animals from Tunisia. *J Glob Antimicrob Resist*. 2022;31:228–235. doi:10.1016/j.jgar.2022.09.007
39. Ren L, Ye J, Zhao B, Sun J, Cao P, Yang Y. The role of intestinal microbiota in colorectal cancer. *Front Pharmacol*. 2021;12:674807. doi:10.3389/fphar.2021.674807
40. Yan D, Qiang Y, Tian T, Lu D, Wu C. The effect of endotoxin on the intestinal mucus layer in non- and post-pregnancy mice. *Front Vet Sci*. 2022;8:824170. doi:10.3389/fvets.2021.824170
41. Rosales IA, Zhou IY, Ay I, Sojoodi M, Sise ME, Gale EM. Imaging kidney inflammation using an oxidatively activated MRI probe. *Kidney Int*. 2024;106:671–678. doi:10.1016/j.kint.2024.05.027
42. Schiepatti A, Sanders DS, Aziz I, et al. Clinical phenotype and mortality in patients with idiopathic small bowel villous atrophy: a dual-centre international study. *Eur J Gastroenterol Hepatol*. 2020;32:938–949. doi:10.1097/MEG.0000000000001726
43. Zhou M, Li X, Liu J, Wu Y, Tan Z, Deng N. Adenine's impact on mice's gut and kidney varies with the dosage administered and relates to intestinal microorganisms and enzyme activities. *3 Biotech*. 2024;14:88. doi:10.1007/s13205-024-03959-y
44. Zhu J, Li X, Deng N, et al. Intestinal mucosal flora of the intestine-kidney remediation process of diarrhea with deficiency kidney-yang syndrome in sishen pill treatment: association with interactions between Lactobacillus johnsonii, Ca(2+)-Mg(2+)-ATP-ase, and Na(+)-K(+)-ATP-ase. *Heliyon*. 2023;9:e16166. doi:10.1016/j.heliyon.2023.e16166
45. Sun Q, Ji YC, Wang Z, et al. Sodium butyrate alleviates intestinal inflammation in mice with necrotizing enterocolitis. *Mediators Inflamm*. 2021;2021:6259381. doi:10.1155/2021/6259381
46. Rigby RJ, Carr J, Orgel K, King SL, Lund PK, Dekaney CM. Intestinal bacteria are necessary for doxorubicin-induced intestinal damage but not for doxorubicin-induced apoptosis. *Gut Microbes*. 2016;7(5):414–423. doi:10.1080/19490976.2016.1215806
47. Lee C, Hong SN, Kim ER, Chang DK, Kim YH. Depletion of intestinal stem cell niche factors contributes to the alteration of epithelial differentiation in SAMP1/YitFcsJ mice with Crohn disease-like ileitis. *Inflamm Bowel Dis*. 2021;27(5):667–676. doi:10.1093/ibd/izaa314
48. Fang L, Shen J, Wu Y, Tan Z. Involvement of intestinal mucosal microbiota in adenine-induced liver function injury. *3 Biotech*. 2025;15:6. doi:10.1007/s13205-024-04180-7
49. Che Q, Luo T, Shi J, He Y, Xu D. Mechanisms by which traditional Chinese medicines influence the intestinal flora and intestinal barrier. *Front Cell Infect Microbiol*. 2022;12:863779. doi:10.3389/fcimb.2022.863779
50. Zhang Z, Yang Y, Zhang Y, Xie G. Co-frequency or contrary? The effects of Qiwei Baizhu Powder and its bioactive compounds on mucosa-associated microbiota of mice with antibiotic-associated diarrhea. *Front Cell Infect Microbiol*. 2024;14:1483048. doi:10.3389/fcimb.2024.1483048
51. Yue B, Zong G, Tao R, Wei Z, Lu Y. Crosstalk between traditional Chinese medicine-derived polysaccharides and the gut microbiota: a new perspective to understand traditional Chinese medicine. *Phytother Res*. 2022;36:4125–4138. doi:10.1002/ptr.7607
52. Li C, Xiao N, Deng N, Li D, Tan Z, Peng M. Dose of sucrose affects the efficacy of Qiweibaizhu powder on antibiotic-associated diarrhea: association with intestinal mucosal microbiota, short-chain fatty acids, IL-17, and MUC2. *Front Microbiol*. 2023;14:1108398. doi:10.3389/fmicb.2023.1108398
53. Fu K, Ma C, Wang C, et al. Forsythiaside A alleviated carbon tetrachloride-induced liver fibrosis by modulating gut microbiota composition to increase short-chain fatty acids and restoring bile acids metabolism disorder. *Biomed Pharmacother*. 2022;151:113185. doi:10.1016/j.biopha.2022.113185